Non-equilibrium in adsorbed polymer layers

2005 J. Phys.: Condens. Matter 17 R63

(http://iopscience.iop.org/0953-8984/17/2/R01)

INSTITUTE OF PHYSICS PUBLISHING JOURNAL OF PHYSICS: CONDENSED MATTER

J. Phys.: Condens. Matter **17** (2005) R63–R99 doi:10.1088/0953-8984/17/2/R01

TOPICAL REVIEW

Non-equilibrium in adsorbed polymer layers

Ben O'Shaughnessy and Dimitrios Vavylonis

Department of Chemical Engineering, Columbia University, New York, NY 10027, USA

E-mail: bo8@columbia.edu and dv35@columbia.edu

Received 13 July 2004, in final form 1 November 2004
Published 20 December 2004
Online at stacks.iop.org/JPhysCM/17/R63

Abstract

High molecular weight polymer solutions have a powerful tendency to deposit adsorbed layers when exposed to even mildly attractive surfaces. The equilibrium properties of these dense interfacial layers have been extensively studied theoretically. A large body of experimental evidence, however, indicates that non-equilibrium effects are dominant whenever monomer–surface sticking energies are somewhat larger than kT, a common case. Polymer relaxation kinetics within the layer are then severely retarded, leading to non-equilibrium layers whose structure and dynamics depend on adsorption kinetics and layer ageing. Here we review experimental and theoretical work exploring these non-equilibrium effects, with emphasis on recent developments. The discussion addresses the structure and dynamics in non-equilibrium polymer layers adsorbed from dilute polymer solutions and from polymer melts and more concentrated solutions. Two distinct classes of behaviour arise, depending on whether physisorption or chemisorption is involved. A given adsorbed chain belonging to the layer has a certain fraction of its monomers bound to the surface, f, and the remainder belonging to loops making bulk excursions. A natural classification scheme for layers adsorbed from solution is the distribution of single-chain f values, $P(f)$, which may hold the key to quantifying the degree of irreversibility in adsorbed polymer layers. Here we calculate $P(f)$ for equilibrium layers; we find its form is very different to the theoretical $P(f)$ for non-equilibrium layers which are predicted to have infinitely many statistical classes of chain. Experimental measurements of $P(f)$ are compared to these theoretical predictions.

(Some figures in this article are in colour only in the electronic version)

Contents

1. Introduction

High molecular weight polymers are extremely surface-active molecules. Even a weak interaction between a single monomer and a surface tends to be magnified into a powerful attraction or repulsion when many of these monomers are linked together to form a polymeric chain. It is a remarkable fact that surfaces contacting even extremely dilute polymer solutions can readily develop very dense polymer layers. Technologies revolving around the properties of either synthetic or biological polymer layers are many and varied, including adhesion [1, 2], coating [3], colloid stabilization [4], fibre reinforced thermoplastics [5, 6], flocculation processes [7], DNA microarrays [8] and biocompatibilization [9]. Motivated both by fundamental questions and by technology, understanding and predicting the structure and formation kinetics of these soft layers is a major concern of polymer science [10]. A crucial aspect of experimental studies is that adsorbed polymer dynamics are typically extremely slow for long chains: an individual chain has many surface stickers and interacts with numerous other chains impeding its motion. Irreversibility and non-equilibrium effects are therefore very common. The subject of this review is experimental and theoretical work on these non-equilibrium effects, and though we consider adsorption from dilute solutions, semi-dilute solutions and melts our main emphasis is neutral homopolymer adsorption from dilute solutions. This is the simplest and most widely studied class.

Polymer–surface adsorption systems are naturally classified according to the mode of adsorption. Roughly, there are two classes: chemisorption and physisorption (see figure 1). The clearest example of irreversibility arises in *chemisorption* (figure 1(b)) where the covalent polymer–surface bonds which develop are often essentially irreversible on experimental timescales. Monomer sticking free energies, ϵ, have values typical of covalent bonds which

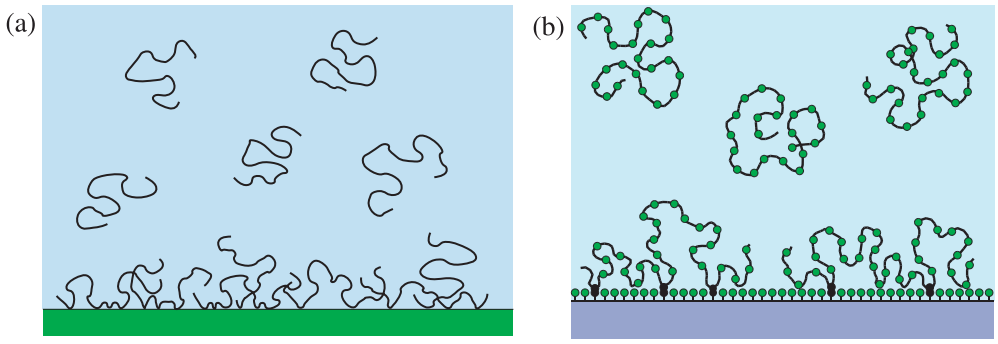

Figure 1. (a) Schematic diagram of physisorption from a fluid polymer phase onto a surface. Adsorbed chains consist of loops, tails and sequences of bound monomers ('trains'). When non-equilibrium effects become important, layer structure depends on kinetics of adsorption. This review addresses physisorption from dilute solutions in sections 2–4 and physisorption from melts in section 6. (b) As in (a) but for chemisorption. In this case chains carry reactive groups which can form covalent bonds (shown black) with a functionalized surface. Chemisorption from dilute solutions is reviewed in section 5 and from concentrated solutions in section 6.

are one to two orders of magnitude greater than kT. Chemical adsorption is employed in various technologies where polymers are attached by chemical reactions to solid surfaces either from a polymer melt as in the reinforcement of polymer–polymer or polymer–solid interfaces [2, 6, 11, 12], or from solution as in colloid stabilization by chemically grafting polymers onto particle surfaces [13–15].

What is less obvious is why non-equilibrium effects are so widely observed in *physisorbing* systems, even for rather weak sticking energies. Available experimental evidence suggests that irreversibility effects become important as soon as ϵ becomes somewhat larger than kT. For example the experiments by Schneider *et al* [16, 17] for polymethylmethacrylate (PMMA) adsorption onto oxidized silica via hydrogen bonding in dilute CCl_4 solutions ($\epsilon \approx 4kT$) show essentially frozen-in adsorbed chain configurations. Large physisorption sticking energies ($\epsilon > kT$) originate in hydrogen bonding or other dipolar forces, dispersion forces or attractions between charged groups. Metal and silicon-based surfaces are usually oxidized and many polymer species form strong hydrogen bonds with the surface oxygen or silanol groups [18, 19]. Biopolymers such as proteins and DNA attach tenaciously to many surfaces due to their many charged, polar and hydrophobic groups [8, 9, 20]. Since hydrogen bonds, for instance, typically have energies of several kT [21, 22], it is apparent that strong physical bonds are very common. This suggests that whether physical or chemical bonding is involved, for long chains irreversible effects may in practice be the rule rather than the exception.

To understand non-equilibrium layers, one must identify how they differ from equilibrium layers. The theory of fully equilibrated layers is far more advanced, at both the mean-field [23] and scaling [24–31] levels of description. A main result of these theories is expressions for the decay of the monomer density profile as a function of the distance z from the surface. For adsorption from dilute solutions for example, in the scaling picture originally developed by de Gennes [24, 25], Eisenriegler *et al* [26, 27], and de Gennes and Pincus [28], each adsorbed chain has sequences of surface-bound monomers (trains) interspersed with portions extending away from the surface (tails and loops of size s) with distribution $\Omega(s) \sim s^{-11/5}$ [29–31] leading to a self-similar density profile $c(z) \sim z^{-4/3}$. Experimentally, the existence of an extended diffuse layer is well established by a large number of neutron scattering [32–37] and neutron reflectivity [38–40] studies. However, a universally accepted quantitative

test of the predicted density profiles has been difficult to achieve, both due to intrinsic limitations of the experimental techniques [41] and to the asymptotic nature of many of the theoretical results which are valid in the limit of very long chains. Furthermore, for experiments specifically directed at equilibrium, ensuring that equilibrium conditions are realized is difficult when the very non-equilibrium effects one wishes to avoid are poorly identified.

Understanding the origin of the observed deviations from equilibrium for weakly adsorbing systems in dilute solutions is a major unresolved puzzle in polymer science. At present it is unclear how universal these non-equilibrium effects may be. Various effects have been speculated to play important roles. Kremer [42] and de Gennes [43] have suggested that if the solution temperature is below the polymer melt glass transition temperature glassy effects may onset at the interface where polymer densities are similar to those of melts. Interactions with the surface might further enhance glassiness. Chakraborty and co-workers [44–47] suggested flattened-down chains experience strong kinetic barriers due to local steric constraints which drastically slow down dynamics. Ideas related to slow cooperative motions, mutual pinning, development of entanglements at the interface and crystallization have been proposed by Johner and Semenov [48], Sommer [49], Granick [50] and Raviv *et al* [51] in a series of comments following a recent theoretical work by Raviv *et al* [52] which interpreted past experiments [53, 54] exhibiting non-equilibrium effects.

In this review we do not attempt an exhaustive review of the vast body of past research work involving strongly physisorbing or chemisorbing polymers at interfaces. Instead, with fundamental issues in mind, our aim is to (i) assemble and classify a number of theoretical ideas and numerical simulations which articulate the community's current level of understanding of equilibrium and non-equilibrium polymer adsorption, and (ii) summarize a number of experimental results which we believe are particularly pertinent and which still demand a theoretical explanation. The emphasis is on the simplest case: adsorption of neutral flexible polymers from dilute bulk solutions. We also review work on irreversible adsorption from semi-dilute bulk solutions and melts, motivated by ideas initiated by Guiselin [55]. Polyelectrolyte solutions, polymers with complex architectures and non-flat surfaces are beyond the scope of the present review.

Physisorption and chemisorption will be carefully distinguished. These are characterized by very different values of the local monomer–surface association rate, Q (see figure 2). In physisorption, monomer attachment is usually essentially diffusion limited, $Q = C/t_a$, where t_a is the monomer relaxation time and C is a system-dependent constant of order unity [56]. Chemisorption is normally much slower [56–58] with Q values typically eight or more orders of magnitude smaller than those of physisorption. The origin of this difference is that chemical bond formation usually involves a large activation barrier (see figure 2). Similarly, desorption rates after chemisorption are usually very small and can be ignored. The effect of desorption on physisorbing systems is more subtle and is discussed in section 4. The above two classes naturally lead to very different adsorption kinetics. This is analogous to *bulk* polymer–polymer reaction kinetics where, depending on Q, polymer length N, and solvent conditions, the kinetics are described by one of a range of 'diffusion-controlled' and 'mean-field' kinetic regimes [58–61]. Such regimes also arise for end-adsorbing polymers [56, 57, 62–67].

In section 2 we briefly review the equilibrium picture for dilute solutions and in section 3 we discuss experimental evidence for non-equilibrium departures from this picture. Theoretical work related to physisorbing non-equilibrium layers from dilute solution is reviewed in section 4. We move to chemisorption, again from dilute solution, in section 5. Section 6 addresses irreversibility effects involving melts and semi-dilute solutions. We conclude with a brief discussion of the experimental and theoretical outlook.

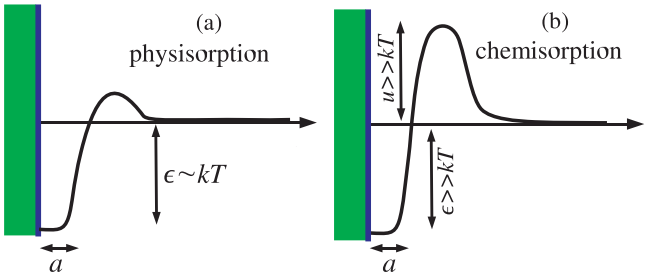

Figure 2. The two broad classes of polymer adsorption, physisorption and chemisorption, have very different values of the parameter Q, the local monomer–surface association rate. Q can be thought of as the conditional monomer–surface sticking probablity per unit time, given that the unattached monomer contacts the surface. Though many systems are in practice mixtures of chemisorption and physisorption, a simplified view of monomer free energy as a function of distance between monomer and surface is shown. (a) For physisorbing polymers, the activation barrier is very small and monomer–surface association is very likely upon contact, i.e. Qt_a is of order unity, where t_a is the monomer relaxation time. When the sticking energy ϵ exceeds a few kT, experiment indicates that chains need large amounts of time to escape the surface, presumably due to complex many-chain effects. (b) Chemisorption typically involves a large activation barrier, $u \gg kT$. Many monomer–surface collisions are needed to traverse this barrier, $Qt_a \ll 1$. The adsorbed state is also usually strongly favoured, $\epsilon \gg kT$.

2. Adsorption from dilute solutions: the equilibrium picture

2.1. Structure of equilibrium layers

This section briefly outlines some central results of equilibrium theories of adsorbed polymer layers. Much more extensive reviews can be found in [41, 68–71]. In the scaling picture developed mainly in the 1980s [24–28], each adsorbed chain consists of surface-bound monomers and large loops and tails generating a monomer density profile $c(z)$ as a function of distance from the surface, z. Eisenriegler *et al* [26–28] showed that very close to the surface, in the 'proximal' region, the density decays as a power law, $c(z) \sim z^{-m}$, where the critical exponent $m \approx 1/3$ represents competition between surface-sticking energy gain, chain entropy, and excluded volume interactions. The proximal region decay law crosses over to de Gennes' 'self-similar grid' regime [24, 25, 28], $c(z) \sim z^{-4/3}$, beyond a certain distance $h_{\rm prox}$. For $z > h_{\rm prox}$ the polymer layer can be thought of as a semi-dilute solution with continuously varying local concentration $c(z)$. In this region the correlation length measuring the range of excluded-volume interactions, $\xi = a^{-5/4}c^{-3/4}$, is proportional to the distance from the surface, z, since this is the only relevant length scale: $\xi \approx z$. Here a is defined to be the monomer size. Expressing ξ in terms of c leads to[1]

$$a^3 c(z) \approx \begin{cases} (a/h_{\rm prox})\,(a/z)^{1/3}, & a < z < h_{\rm prox} \\ (a/z)^{4/3}, & h_{\rm prox} < z < R_{\rm F} \end{cases} \qquad h_{\rm prox} = a\,kT/\epsilon,\ R_{\rm F} = aN^{3/5}. \tag{1}$$

Unless the bulk polymer concentration, c, is extremely small [72], then the equilibrium layer height is of the order of the Flory bulk coil radius $R_{\rm F}$ as indicated in equation (1). In this same range of c the adsorption isotherm exhibits a large plateau, i.e. surface coverage Γ is weakly dependent on c.

[1] The cross-over distance $h_{\rm prox}$ and the prefactor in the proximal region density law can be determined by demanding (i) a smooth cross-over at $h_{\rm prox}$ and (ii) the osmotic free energy per unit area, $\int_a^{R_{\rm F}} {\rm d}z\, kT/\xi^3$, balances the sticking free energy per unit area, $\epsilon\, a\, c(a)$.

Even in weakly adsorbing polymer systems, e.g. adsorption through weak van der Waals interactions, the value of ϵ is usually of order kT. By studying the adsorption/desorption transition in binary solvent mictures, van der Beek *et al* [18] estimated the sticking energies per monomer of many typical flexible polymers onto silica and alumina surfaces from organic solvents to lie in the range 0.5–6kT. Hence the width of the proximal region is typically of the order of the monomer size, $h_{\text{prox}} \approx a$, and a clear signature of the proximal region is hard to probe experimentally. In the following we consider ϵ of order kT or larger. We remark that the net monomer free energy of adsorption ϵ includes both the 'stickiness' a monomer feels for the surface, but also the entropic disadvantage due to constraining local orientational degrees of freedom upon contact with the surface. Thus, crudely speaking, one can say the stickiness contribution must exceed a critical value ϵ_c representing the entropic disadvantage before a monomer can adsorb. Computer simulations show ϵ_c is of order kT and is lattice dependent [27]. The real situation is more complex, with various contributions from electronic and structural factors such as solvent molecule entropy effects, etc [21].

The density decay law of equation (1) reflects a power law distribution of loop and tail sizes. Neglecting differences between loops and tails and the details associated with the proximal region, then the loop size distribution per surface site is [29–31]

$$\Omega(s) \approx a^{-2} s^{-11/5}. \tag{2}$$

Beyond this, Semenov and Joanny [31] showed that the inner region of the layer, $z < z^* \equiv aN^{1/2}$, is dominated by loops while the outer region, $z > z^*$, is dominated by tails; the resulting density profile obeys a $z^{-4/3}$ law above and below z^*, respectively, but with different numerical prefactors. Support for the scaling conclusions of equations (1) and (2) is provided by Monte Carlo simulations of Zajac and Chakrabarti [73], de Joannis *et al* [74, 75], and Cifra [76]. These produce a density decay consistent with the $z^{-4/3}$ law for long chains. Zajac and Chakrabarti [73] additionally report agreement with equation (2).

Complementary to the scaling approach outlined above has been the numerical lattice model of Scheutjens and Fleer (SF) [77, 78]. This is a self-consistent mean field theory which averages excluded volume interactions and thus treats self-avoidance in an approximate manner. This approximation however allows numerical solutions for the density profile and for the loop and tail distributions and can additionally describe chains of finite length. The mean field description becomes more accurate for solvents near the theta temperature (a common case) where self-avoidance is a weak perturbation except for the longest loops and tails. The existence of the loop- and tail-dominated regions of the layer was in fact first established by the SF model [78, 79]. The layer height in the SF theory scales as $h \sim N^{1/2}$ [77, 78] while the density profile decays as $c(z) \sim z^{-2}$ (for sufficiently long chains), different to the $z^{-4/3}$ decay predicted by the scaling approach, as shown by van der Linden and Leermakers [80]. *Analytical* mean field solutions for the density profile in the limit of very long chains were derived within the ground-state dominance approximation [81] by Jones and Richmond [82]. Going beyond the ground state dominance approximation, Semenov *et al* [23] subsequently generalized this approach to account for finite length effects to leading order and analytically describe the different contributions of loops and tails to the density profile. They found that loops dominate for $z < z^*_{\text{MF}} \equiv aN^{1/3}$ while tails dominate for $z > z^*_{\text{MF}}$, similarly to the scaling approach of Semenov and Joanny [31]. These new methods have revived interest in analytical and numerical mean field approaches to polymer adsorption [83–89].

Turning now to experiment, the fundamentals of polymer adsorption at the solid/liquid and air/liquid interface have been studied in a vast number of experiments. Research prior to 1993 is reviewed in the book by Fleer *et al* [41]. Given the strong evidence for nonequilibrium effects (see below), in general one should be very cautious when comparing experimental

findings to equilibrium expectations. Overall, experiment is consistent with the general trend predicted by equilibrium theories regarding structure of the polymer layers which were studied, although the fine differences between the mean field and scaling pictures are hard to distinguish. Very briefly, measurements of the layer's surface bound monomer fraction as a function of total adsorbed amount and molecular weight (MW) by techniques such as NMR [90, 91], ESR [92, 93], or infrared spectroscopy [94] give results fairly consistent with the predictions of the SF theory [41]. The thickness, $h_{\rm exp}$, of polymer layers has been probed as a function of chain length by hydrodynamic methods [41, 95–97], ellipsometry [98], and the surface force apparatus [99]. Depending on the method, $h_{\rm exp}$ is proportional to a certain moment of the density profile and many existent measurements are compatible with a power law, $h_{\rm exp} \sim N^{\alpha}$. Certain studies have favoured the SF theory predictions [41, 96] while others support the scaling predictions [97, 99]. For flexible polymer species the total surface coverage Γ as a function of bulk concentration is found to be very weakly dependent on the polymer concentration in the bulk except for very dilute solutions, in qualitative agreement with both the scaling and the SF theories [41]. For a given bulk concentration, measurements of Γ as a function of N in good solvents typically show a weak dependence on chain length for large N [41]. This is consistent with the SF and scaling theories which predict $\Gamma \sim \int_a^h {\rm d}z\, c(z)$ is dominated by the lower, N-independent limit.

Small angle neutron scattering (SANS) and neutron reflectivity have been used to probe the density profile. These experiments established the existence of a diffuse extended layer but at present there is no general agreement as to the exact form of the density decay. A technical difficulty intrinsic to SANS, as discussed in [41], is its limited sensitivity to the more dilute regions of the layer. Neutron reflectivity experiments are also often ambiguous, since multiple density profiles can be fitted to the same data. The SANS experiments of Auvray and Cotton [35] and Hone *et al* [37] are consistent with the $z^{-4/3}$ scaling law. However, the results of Hone *et al* could also be described by an exponential profile (see also [32]). SANS experiments by Cosgrove *et al* [33, 34] do not support the scaling predictions, but are more consistent with the SF theory. Other SANS studies by Rennie *et al* [36] are inconsistent with both scaling and SF predictions, while neutron reflectivity experiments of Lee *et al* [38, 39] and Sun *et al* [40] have generated data consistent with the scaling predictions.

2.2. Single-chain statistics and the equilibrium distribution of bound fractions

So far this section has discussed many-chain layer properties. Equally important, and characteristic of the layer-forming processes, are properties of *individual* surface-adsorbed chains in the layer. What is the spectrum of configurations of individual chains? According to the scaling picture, a typical chain has $ND(s)$ loops of length s or greater, where $D(s) \equiv \int_s^{\infty} {\rm d}s'\, \Omega(s') \sim s^{-6/5}$ after using equation (2). Semenov and Joanny [100] argue that because of screening effects these are essentially independent blobs and their 2D spatial extent parallel to the surface is $[ND(s)]^{1/2} a s^{3/5} = aN^{1/2}$. This occurs for all scales s; in particular, a given chain has of order one loop of length $N^{5/6}$, also of size $aN^{1/2}$. Hence a typical chain has a lateral size of order $aN^{1/2}$, the ideal result (to within logarithmic corrections [100]).

A special role is played by another single-chain property, directly reflecting the degree to which individual chains are bound to the surface. This is the probability distribution $P^{\rm eq}(f)$ that a chain has a fraction f of its monomers touching the surface. This property plays a central role in this review, since its features closely reflect whether irreversible effects matter or not. In two independent Monte Carlo studies by Wang and Rajagopalan [101] and Zajac and Chakrabarti [73] an equilibrium distribution was found with a single peak at a value of f of order unity. To our knowledge, $P^{\rm eq}(f)$ has not been calculated analytically, at least at the

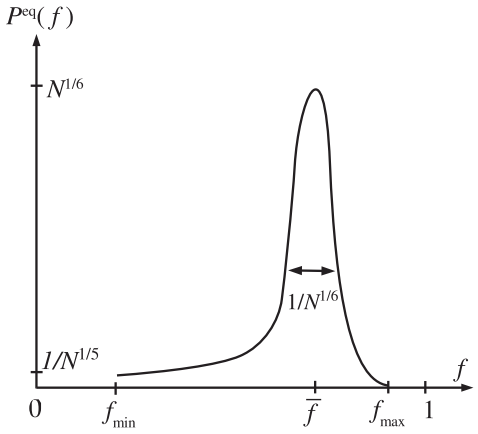

Figure 3. Equilibrium probability distribution P^{eq} of chain bound fraction, f, in good solvents. For very long chains the distribution is sharply peaked at a value $\bar{f}$ of order unity. For realistic values of N the distribution is rather broad.

scaling level. In order to compare equilibrium predictions with experimental measurements of bound fractions in non-equilibrium layers in later sections, we have calculated $P^{eq}(f)$ by relating an adsorbed chain to a 1D unidirectional walk combining an initial tail, a sequence of intermediate steps, and a final tail. The result, which is derived in the appendix and is shown in figure 3, reads

$$P^{eq}(f) \approx \frac{N^{-1/5}}{(f_{max}-f)^{11/5}}\,\rho\left[(f_{max}-f)N^{1/6}\right], \qquad \rho[x] \to \begin{cases} 1 & (x \gg 1) \\ 0 & (x \ll 1). \end{cases} \tag{3}$$

This agrees qualitatively with the numerically measured distribution of [73, 101]. Here $\rho[x]$ is a scaling function which cuts off the distribution at a small-scale-dependent parameter of order unity, f_{max}. The value of f_{max} is determined by the small loops with length $\sim a$, whose number is $\sim N$ per chain. The mean value of the distribution, $\bar{f}$, is located at $\sim f_{max} - N^{-1/6}$. The fluctuations around the mean are due to the mass in long loops of length $N^{5/6}$. There is order one such loop per chain and this diminishes $\bar{f}$ by an amount of order $N^{-1/6}$. Equation (3) has a tail at small f which describes a small population of chains, a fraction of order $N^{-1/5}$ of the total, with f values far removed from the mean: these are the chains with tails [31] of length up to order N which determine the layer height $\approx aN^{3/5}$. Notice in figure 3 we indicate that the distribution changes behaviour at a minimum value, f_{min}, which is also of order unity (to within logarithmic corrections in N [100]). The value of f_{min} is determined by the largest loop or tail size in the layer, expressions for which have been derived by Semenov and Joanny [100]. We note that chains with $f < f_{min}$ values do exist but their number is predicted to be much smaller [100]. For a typical value $N = 1000$, one has $N^{-1/6} \approx 0.32$ and thus the distribution is in practice rather broad. Broadening effects in theta solvents are expected to be even stronger.

3. Dynamics of adsorbed polymers and evidence for non-equilibrium layers

The most direct evidence for deviations from the equilibrium picture derives from experiments on the kinetics of adsorbed polymers. In this section we review analytical and numerical studies of equilibrium layer kinetics and then we proceed to review experiments showing deviations from equilibrium. Particularly revealing experiments have been those probing bulk-layer exchange kinetics.

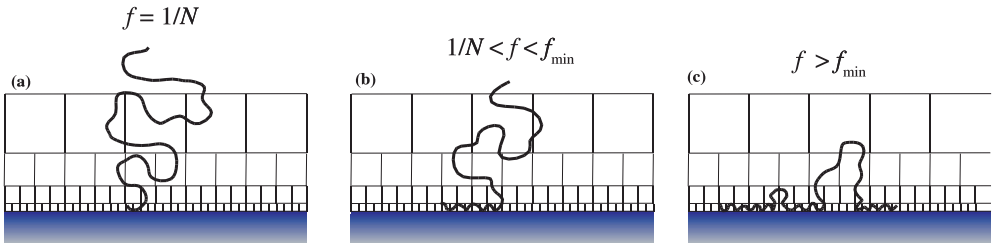

Figure 4. Schematic of new chain adsorption in an equilibrium polymer layer (shown as a self-similar grid) as described in [102]. (a) Entry: a bulk chain reptates into the layer and makes a first attachment to the surface. (b) Spreading: the incoming chain establishes an increasing number of contacts with the surface. (c) A typical adsorbed chain configuration is adopted, consisting of trains, loops and tails. A similar picture was used in [100]. Chain desorption follows the same path in the reverse order.

3.1. Theories of dynamics in equilibrium layers

Compared to static properties, much less is established theoretically about equilibrium dynamics. These have been studied for good solvents by de Gennes [43, 102–105], Semenov and Joanny [100], and Baschnagel *et al* [106] for bidisperse solutions. The picture emerging from these works is that the layer of bound chains has a certain characteristic equilibration time $\tau_{\rm eq}$. This can be thought of as the time after which the chains following the distribution $P^{\rm eq}(f)$ of figure 3 are completely reshuffled among themselves. The exchange of chains between the bulk and the layer was predicted to be a slower process due to the fact that incoming and outgoing chains have to pass through unfavoured configurations having a small fraction of bound monomers (see figure 4). de Gennes assumed reptation dynamics (i.e. entangled layers) and found the longest relaxation time of the layer to scale as [102, 104, 105]

$$\tau_{\rm eq} \approx t_{\rm s} N^3 \qquad \text{(entangled layers)}. \tag{4}$$

Here $t_{\rm s}$ is the relaxation time of an adsorbed monomer which, due to wall–polymer interactions, may be much larger than the corresponding time in the bulk, $t_{\rm a}$ [107]. Semenov and Joanny [100] assumed unentangled layers and Rouse–Zimm dynamics and obtained $\tau_{\rm eq} \approx t_{\rm a} N^2$ (in their work $t_{\rm s} \approx t_{\rm a}$ was assumed).

In equilibrium, layer and bulk chains desorb and adsorb at the same average rate, respectively. In de Gennes' picture bulk chains adsorb in two stages (see figure 4). During the first 'entry' stage, the bulk chain overcomes the excluded-volume barrier presented by the layer's loops and tails and makes its first contact with the surface, i.e. $f = 1/N$. During a second 'spreading' stage the chain continues to make an increasing number of surface contacts, f increases up to $f_{\min}$, and the chain becomes part of the bound layer. When entry is rate limiting he found that the mean lifetime of an adsorbed chain before its desorption is $\tau_{\rm ex} \approx t_{\rm a} N^{3.7}/\phi$, where ϕ is the volume fraction of polymer in the bulk. Semenov and Joanny [100] described the dynamics using a similar picture, but assuming unentangled layers and Rouse–Zimm dynamics. They obtained a slighlty different chain lifetime, $\tau_{\rm ex} \approx t_{\rm a} N^{2.42}/\phi$ (to within logarithmic corrections).

Note that the exchange timescale, $\tau_{\rm ex}$, has a weak power law dependence on N rather than exponential because the incoming/outgoing barrier is small. The scaling $\tau_{\rm ex} \sim 1/\phi$ reflects the linear dependence on concentration of the rate of chain arrival at the surface. Note also that even for the highest dilute solution concentrations, $\phi = \phi^*$, where $\phi^* \equiv N^{-4/5}$ is the chain overlap threshold concentration [81], one still has $\tau_{\rm eq} \ll \tau_{\rm ex}$. A prediction of the above works is that chain desorption into pure solvent, $\phi \to 0$, is extremely slow, which is well established experimentally [108].

Now suppose one starts with a layer of labelled chains in equilibrium and replaces the bulk solution with identical but unlabelled chains of the same concentration at $t = 0$. An important prediction of the above theories is that the decay of the surface coverage of labelled chains, Γ, is a simple exponential for all times [43, 100]:

$$\Gamma(t) = \Gamma(0)\mathrm{e}^{-t/\tau_{\mathrm{ex}}}. \tag{5}$$

An implicit feature of equation (5) is that there is a single observed desorption rate since $\tau_{\mathrm{ex}} \gg \tau_{\mathrm{eq}}$, i.e. the desorption process is slow enough to sample an average over all equilibrium chain states in the layer. Note that this result in fact assumes a given desorbed labelled chain does not readsorb, i.e. memory is lost instantly. Experimentally, this necessitates a mixing process in the bulk to dilute the desorbed chains. In the absence of such mixing diffusion returns a desorbed chain to the surface repeatedly, an effect which can lead to non-exponential decay [60, 109, 110].

The kinetics of polymer layer build-up starting from empty or 'starved' surfaces is more complex and has been considered in [43, 100, 102, 111].

3.2. Dynamics of adsorbed polymer layers: Monte Carlo simulations

This sub-section provides a brief review of numerical Monte Carlo simulations of dynamics in many-chain polymer layers in contact with dilute solutions (for dynamics of single chains see [112–116]). The simulations reported here did not include hydrodynamic interactions. The main results of the simulations by Wang *et al* [101, 117] are qualitatively in agreement with the theoretical picture of the previous subsection. They found that the lateral dynamics of adsorbed chains up to $N = 100$ are consistent with Rouse dynamics. For sufficiently sticky surfaces ($0 < \epsilon \leqslant 1.5kT$ with $\epsilon_{\mathrm{c}} = 0.5kT$) the value of τ_{ex} was found to be much larger than the lateral relaxation time, even though the scaling dependence on N was the same. This should be contrasted with the Semenov and Joanny prediction that the two exponents differ by a small value, 0.42. Wang *et al* observed non-exponential exchange kinetics arising from readsorption of desorbed chains.

Lai [113, 118] studied the layer dynamics as a function of ϵ for $N \leqslant 80$ and interestingly found that for $\epsilon \gtrsim 1kT$ (with $\epsilon_{\mathrm{c}} \approx 0.9kT$) the lateral chain dynamics started to slow down and to approach apparently glassy dynamics at $\epsilon \approx 4kT$. This result was claimed to be valid despite an omission in the implemented algorithm [113, 119]. This report is important since it indicates that the value of ϵ is crucial in polymer adsorption.

Zajac and Chakrabarti [120] studied the dynamics for $N = 100$ and 200 and $\epsilon+\epsilon_{\mathrm{c}} = 1.8kT$ near and above $\phi = \phi^*$. Their algorithm involved unphysical reptation moves in order to speed up the dynamics. In equilibrium they found a distribution of bound fractions similar to the one of figure 3 and observed that the internal dynamics of reshuffling of chains between different f values is complex. The timescale for the exchange of adsorbed chains by bulk chains was found to be slower than internal equilibration processes. Simple exponential exchange kinetics were observed as in equation (5).

Takeuchi [121] also used the Monte Carlo method with extra reptation moves. For surfaces with $\epsilon \approx 1.6kT$ he observed exponential exchange kinetics while for $\epsilon \approx 0.9kT$ readsorption effects were important leading to non-exponential exchange kinetics.

3.3. Experiment: departure from equilibrium picture

The first experimental studies of exchange kinetics on flexible polymers were performed by Pefferkon *et al* [122–125] using radioactive labelling techniques. One study [122, 124, 125] involved labelled polyacrylamide (PAM) in water adsorbed through hydrogen bonding onto

aluminol-grafted glass beads. The beads were exposed to a dilute solution of labelled PAM for approximately 30 min until time-independent coverage was achieved. The labelled solution was then replaced by a dilute unlabelled PAM solution of varying concentration c and the amount of labelled PAM which remained adsorbed, Γ, was monitored as a function of time as shown in figure 5(i). An interesting result of this experiment was that the exchange rate per labelled chain, shown in figure 5(ii), was *time dependent* and reached a constant value after a cross-over period of ≈ 300 min which was approximately the same for every c. This asymptotic rate was found to increase linearly with c, as shown in figure 5(iii). The observed spectrum of exchange times disagrees with equation (5) and this can be interpreted in many ways as follows.

(i) The observed non-exponential exchange kinetics is a signature of non-equilibrium. Pefferkorn *et al* [122, 124] argued that the interface is populated with a spectrum of different frozen or slowly changing configurations and, consequently, different kinetic properties. (They proposed that the layer consists of a flat sublayer of tightly bound chains which exchange slowly, plus a less tightly bound population which exchange more rapidly.)

(ii) The layer is not in equilibrium when the exchange experiment starts but it equilibrates after $\tau_{\rm eq} \approx 300$ min which is larger than the layer's preparation time. The asymptotic exchange rate then becomes constant and equal to $1/\tau_{\rm ex}$. The fact that asymptotically $\tau_{\rm ex} \sim 1/c$ as seen in figure 5(iii) and the fact that $\tau_{\rm ex} > 300$ min as can be seen in figure 5(ii), are consistent with this interpretation and the theories reviewed in subsection 3.1. Assuming reptation dynamics, equation (4), and given $N \approx 1400$, this implies a relaxation time of adsorbed monomers of order $t_s \approx 10^{-5}$ s. This is much larger than monomer relaxation times in the bulk, $t_{\rm a} \approx 10^{-10}$ s.

(iii) The layer is in fact in equilibrium but its exchange kinetics and internal equilibration processes are much more complex than assumed by existent theories, at least for this system. For example, if the equilibrium $P^{\rm eq}(f)$ is very broad and chains with different f values have very different exchange times, then the initial drop in Γ will be due mainly to the most rapidly desorbing chains if their desorption times are less than $\tau_{\rm eq}$.

Issues related to surface density of aluminol groups, polydispersity, and effect of pH (this experiment was performed at pH $= 4$ where PAM is neutral while many of the surface aluminol groups were positively charged [122, 126]) may further complicate the dynamics.

In [123, 124] Pefferkorn *et al* performed an experiment similar to their PAM studies, but for polystyrene (PS) in CCl_4 (under good solvent conditions) adsorbing through hydrogen bonds onto glass beads bearing surface silanol groups. The measured specific exchange rate of labelled chains shown in figure 6 was found to be time dependent for high surface coverages, but independent of time for low Γ. The interpretation [123, 127] was that for small Γ the layer consists of flattened-down chains with identical exchange kinetics. At higher Γ an outer layer of loosely bound chains builds up and one returns to the phenomenology of the PAM case (figure 5) with time-dependent exchange rates.

Systematic experiments on PS exchange kinetics were also performed by the group of Granick. In a series of experiments, Frantz and Granick [128, 129] studied the exchange of adsorbed protonated PS (hPS) by bulk deuterated PS (dPS). Measurements were performed in cyclohexane at the theta temperature of dPS, 30 °C, slightly below the theta temperature of hPS, 34.5 °C [129]. The attractive surface was flat oxidized silicon. Studying desorption in binary solvent mixtures (using a method developed by Cohen Stuart *et al* [18, 130, 131]), it was found that [19, 132] $\epsilon \approx 2kT$. After incubating the surface in dilute hPS solution for different ageing times, the solution was replaced by dilute dPS solution and the adsorbed amount of hPS

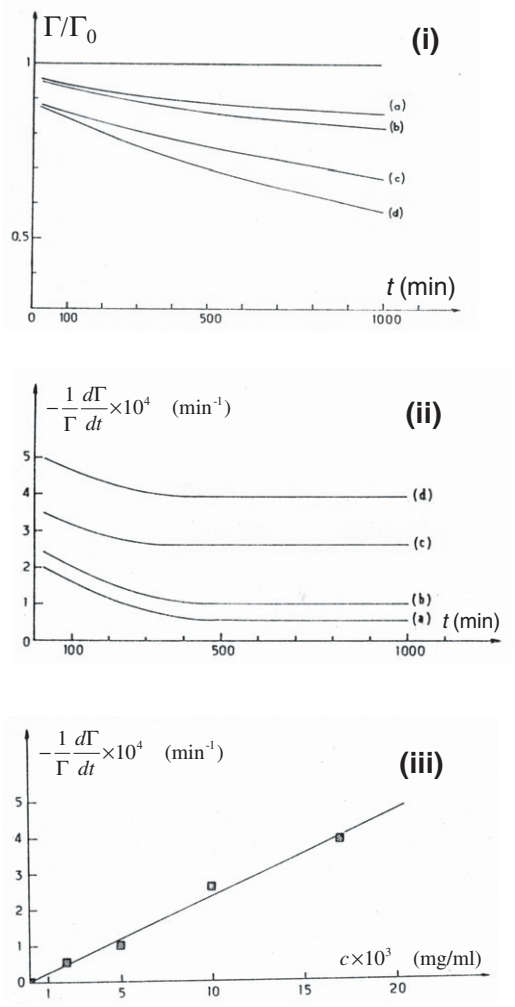

Figure 5. (i) Time dependence of surface coverage Γ of radio-labelled PAM on glass beads in water in the presence of polymer solutions at concentration $c = 2 \times 10^{-3}$ (a), 5×10^{-3} (b), 10×10^{-3} (c), 17×10^{-3} mg ml^{-1} (d). The unlabelled curve at the top is desorption in the presence of pure solvent. Γ_0 is the initial surface coverage. (ii) Specific exchange rate of radio-labelled PAM, from surface to solution, as a function of time for different bulk concentrations as in (i). The rate is time dependent which indicates non-exponential exchange kinetics. (iii) Asymptotic specific exchange rate of radio-labelled PAM as a function of bulk concentration. (Reprinted with permission of John Wiley & Sons, Inc. from [122], Copyright ©1985 John Wiley & Sons, Inc.)

and dPS was monitored as a function of time by measuring infrared adsorption spectra (see figure 7(i)). Similarly to the experiments of Pefferkorn *et al* [123, 124] the exchange rate was time dependent. One sees in figure 7(i) that at long times an apparently exponential regime is reached as in figure 5(ii). The important result however is that the time dependence at *short* times was found to be strongly dependent on the layer's ageing time. The surface coverage of hPS at short times could be fitted by an exponential law, $\Gamma \sim \mathrm{e}^{-t/\tau_{\mathrm{ex}}^0}$. It was found that τ_{ex}^0 reached a constant after ageing times of the order of hours, depending on both N (of order a few thousand) and the concentration of the hPS solution (see figure 7(ii)). This suggests the layer structure was continuously evolving into an equilibrium or metastable state over periods

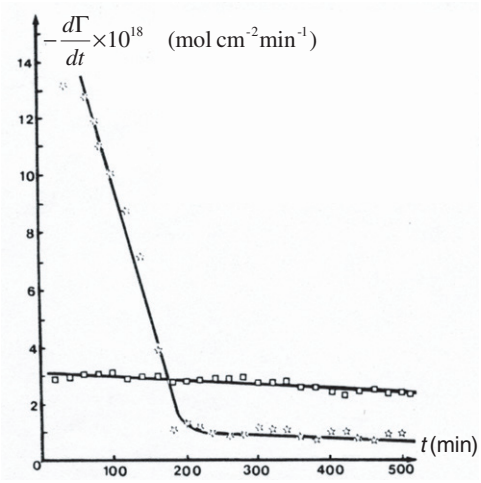

Figure 6. Exchange rate of radio-labelled PS adsorbed on glass beads in CCl_4 as a function of time under different conditions. Squares: $T = 25\,^{\circ}$C, $c = 0.9 \times 10^{-11}$ mol ml^{-1}, initial surface coverage $\Gamma_0 = 3.4 \times 10^{-13}$ mol cm^{-2}. Stars: $T = 35\,^{\circ}$C, $c = 5 \times 10^{-11}$ mol ml^{-1}, $\Gamma_0 = 4.2 \times 10^{-13}$ mol cm^{-2}. (Reprinted with permission from [123]. Copyright 1989 American Chemical Society.)

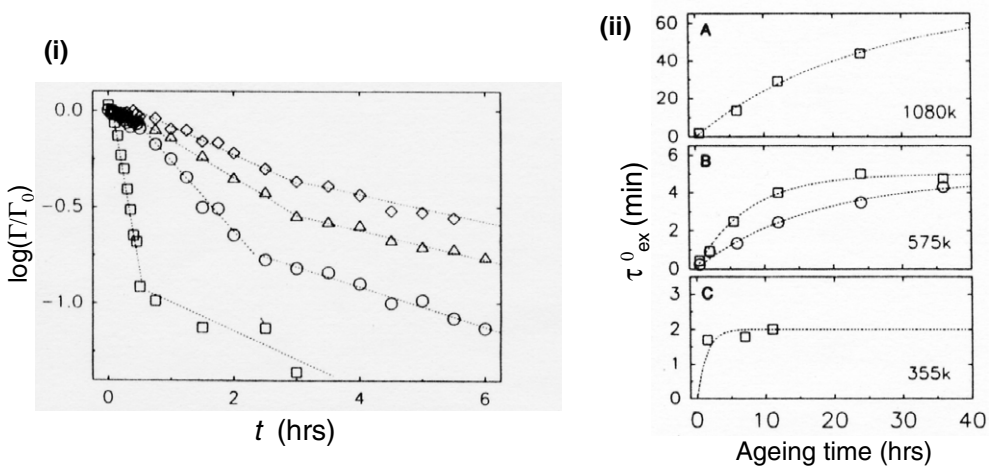

Figure 7. (i) Kinetics of exchange of the adsorbed mass of hPS adsorbed on oxidized silicon in cyclohexane, normalized by the surface excess just before replacing hPS by dPS solution. Different ageing times are shown as follows. Squares, 30 min; circles, 6 h; triangles, 12 h; diamonds, 24 h. The initial decay of Γ can be fitted by an exponential, $\Gamma \sim e^{-t/\tau^0_{ex}}$. (ii) Initial exchange timescale, τ^0_{ex}, plotted against ageing times of the initially adsorbed hPS of various molecular weights. A, MW = 1080 000; B, MW = 575 000; C, MW = 355 000. The MW of dPS is 550 000. Squares and circles represent adsorption from solution concentrations $c = 1.0$ and 0.1 mg ml^{-1}, respectively. (Reprinted with permission from [129]. Copyright 1994 American Chemical Society.)

of hours. The large ageing time value of τ^0_{ex} was found to be exponentially dependent on N for a fixed molecular weight of displacer dPS chains.

The results shown in figures 5 and 7 are at least consistent with initially non-equilibrium layers exhibiting a spectrum of exchange rates, which then age towards equilibrium. A possible

model of these events can be constructed as follows in terms of the chain–surface contact distribution, $P(f)$. According to theories [17, 133, 134] of the non-equilibrium layer, after adsorption onto a very sticky surface $P(f)$ has a much broader distribution than the equilibrium $P^{eq}(f)$. This includes a finite fraction of chains with very small contacts and fast bulk–surface exchange kinetics; it also includes a fraction of order one which has the maximum possible number of contacts, i.e. chains lying fully adsorbed and flattened onto the surface. One would expect these latter may have very large τ_{ex} values. Thus when desorption is measured, the first τ_{ex} values seen are those chains with small f values; as time progresses larger and larger f values have had time to desorb. This is the τ_{ex} spectrum. Only after the layer equilibration time τ_{eq} does the distribution of f values reach the equilibrium $P^{eq}(f)$ of equation (3). This is much less broad, centred on a mean f value corresponding to a τ_{ex} value much greater than τ_{eq}. Thereafter, a single averaged mean exchange time is observed. It should be mentioned, however, that in the experiments of figure 7 this last phase of reaching equilibrium is not manifest; it is possible that this system never reaches a true equilibrium.

In another study by Schneider and Granick [135], the displacement of hPS by dPS adsorbed on oxidized silicon was explored in CCl_4 under moderately good solvent conditions. The adsorption energy was $\epsilon \approx 1.3kT$ [19, 132, 135], measured with the method of [18, 130, 131]. Once again, τ_{ex}^0 was dependent on ageing times, and it took hours for it to reach what might be a plateau. A main difference with respect to the theta solvent case just described above is that at longer times of the order of hours, the exchange rate became essentially zero and no significant exchange could be detected over periods up to 10 h (data not shown). Thus a fraction of order unity of hPS chains remained trapped in the layers, even when the displacer chains dPS chains were much longer than the pre-adsorbed hPS (see figure 8(b)). These findings seem to support a picture where the evolution of the layer during ageing leads to a state containing more and more kinetically trapped chains. This state was reached more rapidly for shorter chains and the trapped fraction depended on the length of displacer chains. The authors of [135] argue that it is unlikely that trapping occurs due to the slight difference between the adsorption energies of hPS and dPS. We note that Pefferkorn *et al* found initial exchange rates of order per hours [123] for a far more dilute system involving PS in CCl_4 adsorbed onto silanol groups (figure 6).

We note that experiments by Dijt *et al* [136] on 'young' PS layers formed in flow from decalin solutions onto silica (at theta solvent conditions where $\epsilon \approx 2kT$ [132, 136]) showed no evidence of significant non-equilibrium effects. These workers used optical reflectometry to measure the surface coverage Γ in mixtures of short (MW $\approx$ 10 000) and long (MW $>$ 100 000) PS chains. Unaged mixed polymer layers with different compositions were generated which led to measurable differences in surface coverage. It was found that layers with the same final composition had approximately the same final surface coverage, independently of adsorption history. This was not true for transient layers whose coverage however relaxed rather rapidly, in times of the order of minutes. At present it is not clear if and how the apparently fast equilibration of Γ is related to the relaxation of chain configurations probed by exchange experiments using labelled chains which appears much slower.

Another widely studied adsorbing polymer is poly(ethylene oxide) (PEO) for which the glass transition temperature (without solvent) is $T_g \approx -41\,^{\circ}C$ and the melting temperature is $T_m \approx 70\,^{\circ}C$ [137, 138]. PEO is thus considerably more flexible as compared to PS which has $T_g \approx 90\,^{\circ}C$ [137]. Dijt *et al* [136] studied mixed layers of long and short PEO chains adsorbed onto silica via hydrogen bonding in aqueous solutions using the same method they used for PS and found fast relaxation dynamics for the coverage of unaged mixed layers. More recently, Fu and Santore [139, 140] and Mubarekyan and Santore [138, 141] have further explored the kinetics of PEO adsorption using TIRF (total internal reflectance fluorescence). Their studies involved adsorption of unlabelled and fluorescently labelled PEO onto silica

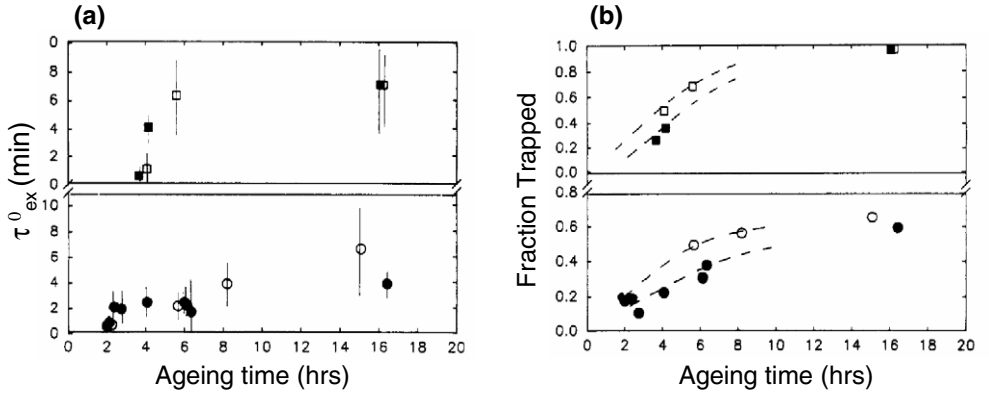

Figure 8. (a) Plot of the initial exchange time constants, τ^0_{ex}, for the displacement of hPS adsorbed onto oxidized silicon in CCL_4 by dPS versus ageing time. Bottom graph (circles): dPS MW = 550 000. Top graph (squares): dPS MW = 87 000. Open (filled) symbols denote hPS MW = 96 400 (MW = 575 000). The diamond indicates a 96 400 hPS/550 000 dPS exchange following a 6 h ageing of a bare surface in pure solvent. (b) Trapped fractions of hPS plotted against ageing times. Symbols as in (a). (Reprinted with permission from [135]. Copyright 1992 American Chemical Society.)

from water, a good solvent, in flow. Microcalorimetry studies [142] indicate $\epsilon \approx 1kT$. It was found [139, 140] that the displacement of short PEO chains by long ones was fast for unaged layers, qualitatively consistent with the findings of Dijt *et al* [136]. However, with increasing chain length and ageing, the exchange kinetics started to slow down and could not be described by a single exponential exchange law as in equation (5) [138, 140]. For long chains a fraction of the layer appeared unexchangeable during the experiment's duration, of the order of hours (this is similar to the trapped fractions observed for PS by Schneider and Granick [135], figure 8(b)). It was found that after a certain maximum ageing time further ageing had no observable effect in the kinetics. The observed ageing effects are summarized in figure 9 where the initial exchange rate is plotted as a function of molecular weight and ageing time. Ageing in these experiments was performed in a pure solvent rather than in contact with the dilute solution. A difference between the findings of the groups of Santore and Granick (for PS) is that Mubarekyan and Santore report an initial exchange rate reaching a plateau value more rapidly for longer rather than short chains. At long times the kinetics could be fitted by a stretched exponential. This may be due to a continuing relaxation of the layer, but also it may be due to the effects of chain polydispersity [140]. Polydispersity effects may be very important in these systems due to the tendency of long chains to displace the shorter ones, since long chains suffer less entropic penalty when immobilized at the surface [106]. In [141] mixed layers of labelled and unlabelled chains were formed and the kinetics of fluorescent chain exchange with unfluorescent bulk chains was studied. Provided the layers were aged for a period of a few hours, an interesting result was that the kinetics were identical irrespective of the adsorption history of the labelled subpopulation. Thus the picture of different classes of chains whose conformation is determined by the time of their arrival on the surface appears inapplicable for this system.

The most direct evidence of irreversible effects has been provided in another series of experiments by Granick's group [16, 17, 143, 144] who followed the adsorption of protonated PMMA (hPMMA) and deuterated PMMA (dPMMA) onto oxidized silicon via hydrogen bonding from a dilute CCl_4 solution (pure PMMA has $T_g \approx 100\,^{\circ}C$). The temperature was

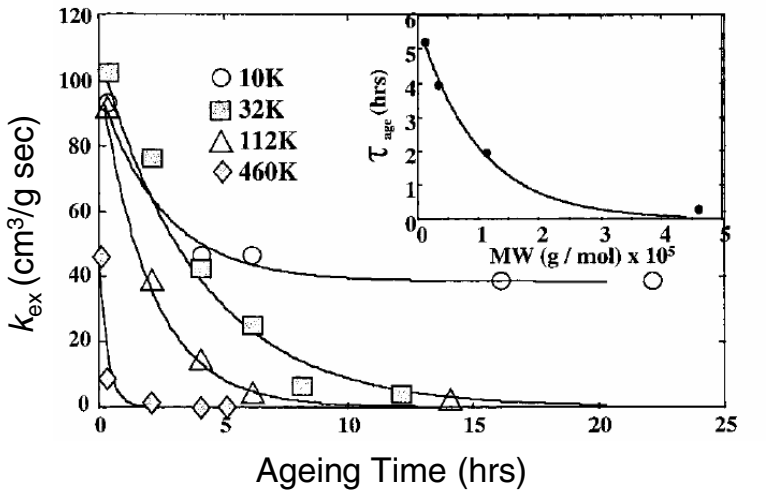

Figure 9. Values of the initial exchange rate, $k_{ex} \approx 1/(\tau_{ex}^0 c)$, for the displacement of labelled PEO chains adsorbed onto silica in water by unlabelled chains of the same MW, as a function of ageing time and MW. The curve through each data set is a single exponential, $k_{ex}(\tau) = k_{ex}(0)e^{-t/\tau_{age}}$, summarizing the layer evolution for each particular molecular weight. The inset summarizes the ageing time constants τ_{age} for the single-exponential fits in the main part of the figure. (Reprinted with permission from [138]. Copyright 2001 American Chemical Society.)

30 °C, slightly above the theta temperature of hPMMA, 27 °C [143]. This is a system with somewhat larger sticking energy, $\epsilon \approx 4kT$ [143]. These PMMA layers exhibited extremely slow exchange rates with bulk chains: for layers of hPMMA aged for ≈1 h and exposed to dPMMA solution, $\tau_{ex}^0 \approx 100$ h was measured, much longer than the duration of the experiment [143]. Infrared absorption spectroscopy was used to measure simultaneously the total coverage Γ and the surface-bound part Γ_{bound} as they evolved in time [16, 17]. This revealed the functional relationship $\Gamma_{bound}(\Gamma)$, which was found to be independent of molecular weight; see figure 10(a). Using deuterium labelling in combination with infrared dichroism measurements they could measure the bound fraction f of chain subpopulations. It was found that early arriving chains had much higher f values than late arrivers, and these f values were frozen in during the experiment's duration. Measuring the distribution of f values among chains they found a bimodal distribution shown in figures 10(b), (c) with two peaks at small and large f, respectively. This is strikingly different to equilibrium layers where the distribution exhibits a unique peak shown in figure 3; for very large N all chains within an equilibrium layer become statistically identical and to within small fluctuations are characterized by the *same* value, $f = \Gamma_{bound}/\Gamma$. The results of other experiments by Soga and Granick [145] studying poly(dimethylsiloxane) (PDMS) adsorbing onto oxidized germanium from CCl_4 were consistent with the existence of a bimodal distribution.

Parallel to the above works on exchange kinetics, evidence for very slow and possibly non-equilibrium behaviour has been gathered in experiments measuring forces between polymer covered surfaces using the surface force apparatus. These systems have been modelled using equilibrium concepts [146–149]. Significant hysteresis effects are, however, common: for PS adsorption onto mica in near-theta solvents, Hu and Granick [150] and Ruths *et al* [151] have observed that following the first compression run the force as a function of surface separation during decompression is different and corresponds to layers of smaller thicknesses. Ruths *et al* observed that force profiles upon recompression did not relax back to the original profile

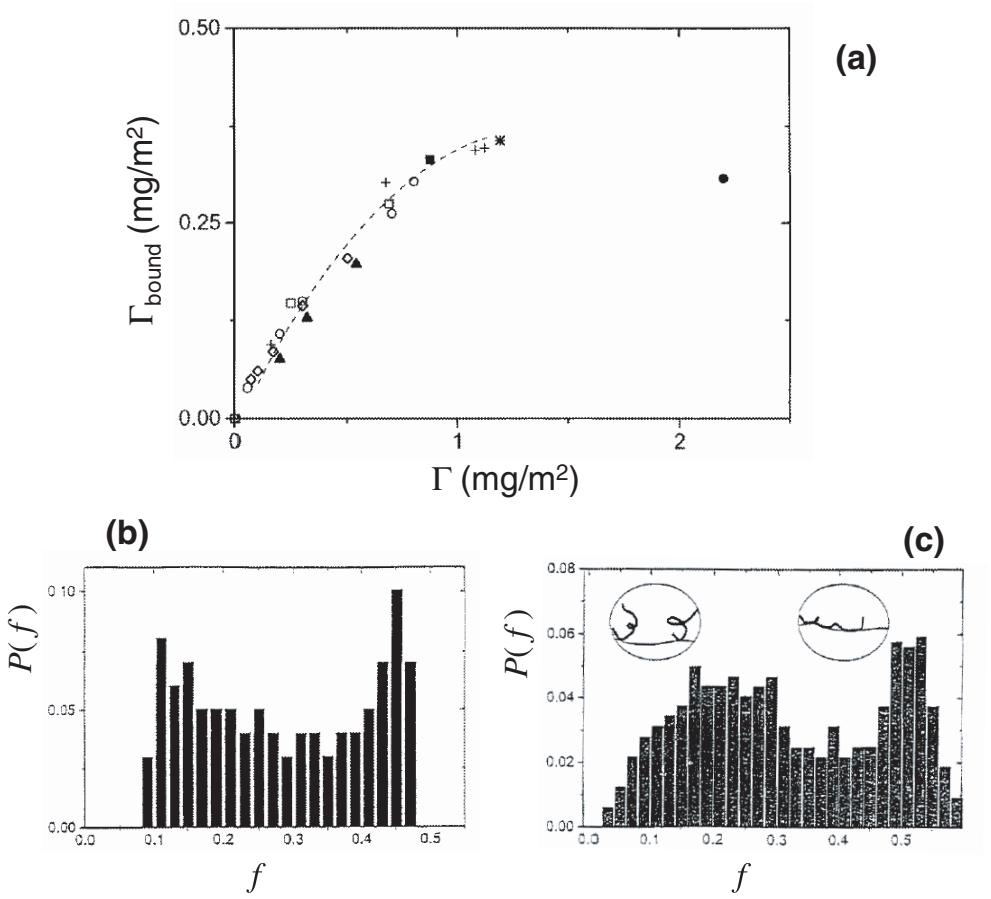

Figure 10. (a) Mass bound by hydrogen bonding to the surface, Γ_{bound}, versus total mass adsorbed, Γ, for PMMA adsorption onto oxidized silicon from CCl_4 at concentration $\phi = 0.01$ mg ml^{-1}. Dashed line: results from uninterrupted adsorption experiments, MW = 107 000. Symbols: results from dosage experiments (see [16, 17]). Open circles, MW = 90 000; diamonds, MW = 107 000; filled squares, MW = 64 000; open squares, MW = 7700; stars, MW = 64 000 at $\phi = 0.08$ mg ml^{-1}; plus signs, MW = 107 000 in toluene solvent; filled circle, MW = 107 000 from semi-dilute solution. (b) Histogram of distribution $P(f)$ of chain bound fractions f, derived from uninterrupted adsorption experiments shown in (a). (c) As in (b) but with $P(f)$ derived from dosage experiments. (Reprinted with permission from [17]. Copyright 1997 IOP Publishing Ltd.)

for days. These workers assigned the observed phenomenology to extremely slow relaxation processes. (For these systems the authors estimate [151, 152] $\epsilon \gtrsim 0.3kT$). Similarly slow dynamics were observed by Ruths *et al* [153] for poly(ethylene–propylene) on lipid coated mica in good solvent.

For the more flexible PEO systems, hysteresis effects are also observed but appear to relax faster. Luckham and Klein [53] and Raviv *et al* [54] studied PEO adsorbed onto mica in toluene, a good solvent (in [52] it was estimated that $\epsilon \approx 0.25kT$ after using the theory of [148] to relate osmotic pressure to sticking energy). The layers were incubated in solution overnight, the two surfaces brought into contact, and the force measured as a function of separation using a surface force balance. The force profile upon decompression or rapid subsequent recompression was

found to be different to the initial profile, describing a layer of a smaller thickness than the one during the first compression. Recovery of the original force profile occurred more rapidly for shorter polymers. Recovery times for the longer polymers (molecular weight 310 000) was of order an hour. Theoretical work by Raviv *et al* [52] assuming irreversibly frozen chain configurations of the compressed layer is consistent with the measured force–distance relationship immediately after compression. Johner and Semenov [48] proposed that a dense phase of PEO nucleates on the surface. There is also evidence, albeit controversial [154, 155], that PEO forms aggregates in solution which adsorb onto surfaces [156, 157]. If so, this could be an important complication in all PEO systems.

Further information on the dynamics of adsorbed polymers in solution arises from experiments on systems which are by their nature far from equilibrium. This includes studies of the kinetic build-up of layers on initially bare surfaces. A recent review of kinetics in such systems is given by Cohen Stuart and de Keizer [108]. Another class of far from equilibrium systems involves the displacement kinetics of adsorbed chains by chains of a different species. Experiments performed by the Granick group [158–161] involved PS adsorbed onto oxidized silica over a period of 1 h in a good solvent (CCl_4), displaced by a more strongly adsorbing polymer: Johnson *et al* [158, 159] studied displacement by PMMA while Schneider *et al* [160, 161] studied displacement by polyisoprene. These studies found that coverage of surviving PS chains, Γ_{PS}, obeyed long time stretched exponential laws, $\Gamma_{PS} \sim e^{-(t/\tau')^{\beta}}$, where τ' was of the order of hours and strongly temperature dependent. Dijt *et al* [162] studied displacement of PS by poly(butyl methacrylate) (PBMA) and poly(tetrahydrofuran) (PTHF), and displacement of PBMA by PTHF. Adsorption occurred on oxidized silicon in decalin solutions. Their results suggested that chain flexibility plays important roles in determining the magnitude of exchange timescales. Finally, evidence for slow relaxation processes in adsorbed polymer layers also comes from ESR measurements by Pan *et al* [163] for adsorption of PS onto porous silica in CCl_4.

4. Theoretical work on non-equilibrium physisorption

In the previous section we reviewed experimental evidence for non-equilibrium effects in polymer layers in solution. In summary it appears that, with increasing ageing, chains adsorbed on strongly attracting surfaces undergo internal relaxation processes and become progressively more attached to the surface and harder to remove. This internal relaxation process becomes slower for even more sticky surfaces, and for systems such as PMMA on oxidized silicon the chains appear to become effectively frozen into configurations which depend on their adsorption history. The universality of the existent observations is unclear.

In this section we review theoretical work addressing these issues. Despite many proposals, the nature of the very slow dynamics is not well understood.

4.1. Single-chain physisorption

Perhaps the simplest problem to attack theoretically is single-chain adsorption in the limit of complete irreversibility of monomer–surface bonds. For physisorption, each attachment is typically very rapid after monomer–surface contact, requiring a small number of monomer–surface collisions. We are not aware of first principles analytical theories addressing this problem which account for the complex polymer hydrodynamics near an interface, subject to an increasing number of surface–polymer bonding constraints. (However, somewhat related issues have been addressed theoretically in the context of chain collapse kinetics in a poor solvent [164].) Ignoring hydrodynamics, one might expect an upper bound on the adsorption

timescale τ_{ads} to be the bulk coil relaxation time τ_{bulk} [81, 165], since the constraints formed by attachments would presumably accelerate the rate of arrival of new monomers onto the surface. However, the validity of even this statement is no longer clear when polymer–surface hydrodynamics are important.

Numerical studies have provided important insight. Shaffer [166] used the bond fluctuation model to study single-chain adsorption on a surface with sticking energy 10 kT. Due to the high cost in computer time hydrodynamic interactions were not included. Since there was no activation barrier for monomer adsorption, his results correspond physically to almost irreversible physisorption. Using $N \leqslant 80$, he found that in the presence of excluded volume interactions (physically corresponding to dilute solution) $\tau_{ads} \sim N^{1.58}$. In the absence of both excluded volume interactions and hydrodynamics (which would correspond physically to the adsorption of a few sticky chains from a non-adsorbing polymer melt matrix), $\tau_{ads} \sim N^{1.5}$. Note that both timescales are weaker powers of N than the corresponding bulk relaxation times [81, 166]. Similar scalings to those of Shaffer were independently obtained by Ponomarev *et al* [167] who used the bond-fluctuation model for $N \leqslant 100$. The kinetics of single chains adsorbing onto strongly attractive surfaces have also been studied by molecular dynamics simulations by van Eijk *et al* [168] and Liu and Chakrabarti [114]

Konstadinidis *et al* [169] used Monte Carlo simulations to study the structure of a single fully and irreversibly collapsed chain on a surface. In the collapsed state, whose nature was dependent on the adsorption kinetics, steric and topological constraints at the monomer level prevented every chain unit from actually touching the surface. The fraction of a flattened chain's monomers which are physisorbed to the surface was measured to be $\omega \approx 0.85$. This should be compared with the value that this simulation would have produced, $\omega \to 1$, if the system were allowed to reach equilibrium by introducing, say, a very small desorption rate. This is because in the limit $\epsilon \gg kT$ the nature of this particular lattice model allows the chain to completely flatten down into a two-dimensional 'pancake' [43, 81].

An important open issue is how to go beyond complete irreversibility and study, for very sticky surfaces, the dynamics of a single chain after flattening down onto the surface. These dynamics are relevant to layer formation on sticky surfaces during the early stages when the layer consists of isolated single chains. In a simple picture, one might expect that for $\epsilon > kT$ monomer relaxation rates are locally slowed down by a Boltzmann factor $\sim e^{(\epsilon+u)/kT}$ associated with local kink formation laterally or normal to the surface (here u is the height of the adsorption potential barrier; see figure 2(b)). However, the scaling with respect to N would remain a power law[2]. On the other hand, dynamics may be more fundamentally modified both by local steric and global topological constraints. Due to local constraints the degree to which a monomer in this flattened configuration can move laterally or desorb is likely to be strongly dependent on the adsorption state of nearby monomers. Thus its motion might necessitate the cooperative motion of its neighbours which introduces kinetic barriers. Chakraborty and co-workers [44–47] studied numerically a one-dimensional Ising model of the effect of such kinetic barriers. For $\epsilon > kT$ stretched exponentials were found in the dynamics of correlation functions. Relaxation times increased with increasing ϵ and in certain cases diverged as ϵ increased towards a value of order kT. These results are similar to those obtained in kinetic Ising models of glasses [175]. They were interpreted to indicate the onset of glassiness in strongly adsorbing systems. The effect of global topological constraints on the dynamics has not been analysed to our knowledge.

[2] For weakly adsorbed chains, this scaling has been measured [170–174] and numerically simulated [112, 115]. In [170, 171] using poly(ethylene glycol) dilutely adsorbed onto self-assembled hydrophobic monolayers, condensed octadecyltriethoxysilane, with $\epsilon \approx 0.5$–$1kT$, simple power laws were measured for the chain's self-diffusivity: $D \sim N^{-3/2}$.

4.2. Many-chain adsorption

Although at present there is little theoretical work addressing the precise nature of the extremely slow dynamics in adsorbed layers, past work has suggested a number of potentially important factors as follows.

(i) Adsorbed monomer relaxation times may be considerably lengthened due to Boltzmann factors $e^{(\epsilon+u)/kT}$ associated with desorption (see figure 2).

(ii) Topological constraints may be important, as suggested in [48, 50, 51, 138]. It is natural to expect that if the equilibrium layer is dominated by loops of the order of the monomer size, then mutual pinning down of chains may become very restrictive. Equilibrium theory does indeed predict that when ϵ reaches values $\sim kT$ or greater most of the mass of a typical chain belongs to such small loops. This hints at a possible transition to more glass-like behaviour at this point.

(iii) Equilibrium theory predicts that for $\epsilon \geqslant kT$, the monomer density at the surface ($z \approx a$) becomes of the order of the density in a polymer melt; see equation (1). Kremer [42] and de Gennes [43] have suggested that if the solution temperature is below T_g for the melt (as it would be, for example, for PS and PMMA at room temperature), glassy effects might onset at the interface where polymer densities are similar to those of melts. Interactions with the surface may further enhance glassiness. Consistent with this picture, increases of glass transition temperatures have been observed for thin polymer melt films deposited onto strongly adsorbing surfaces [176, 177].

(iv) de Gennes [178, 179] suggested that a dense polymer phase may form near the sticky surface for water soluble polymers such as PEO. This would block interfacial chain motion. Johner and Semenov [48] proposed an analogous mechanism for PEO in an organic solvent but this was disputed by Raviv *et al* [51]. Analogous phenomena might occur for other polymers which tend to form crystalline phases. Chain stiffness may also enhance local chain alignment and surface ordering effects.

(v) The dynamics in thin polymer melt films are often much slower than in the bulk, even above T_g [177, 180]. The theory of Semenov [181] and of Semenov and Johner [182] for confined polymer films predicts relaxation times which depend exponentially on molecular weight, similar to the activated reptation model of bulk entangled melts [183–185]. Unlike the unconfined case, Semenov found exponential dependence for even short entangled polymers in the confined situation. Semenov and Joanny [100] proposed that a similar phenomenology might apply to adsorbed polymers in solution.

Most theoretical studies of non-equilibrium effects have considered the limit of complete irreversibility upon attachment. This is directly relevant to more sticky systems such as PMMA on oxidized silicon [16, 17]. Barford *et al* [186] studied irreversible physisorption, motivated by experiments on polyelectrolyte adsorption. Since the limit of high salt concentration was considered, this analysis is also relevant to neutral polymers. The build-up of the polymer layer profile $c(z, \Gamma)$ was followed as a function of increasing surface coverage Γ. An incremental increase in adsorbed amount $d\Gamma$ contributes a change in density $dc(z, \Gamma)$ whose form was determined by numerical solution of self-consistent mean-field equations in which the excluded-volume repulsion due to earlier arriving chains was assumed to be represented by a *fixed* external field. Physically, this models a situation where new chains are irreversibly frozen in after exploring the phase space which was available upon their arrival. The incremental profiles were integrated up to the saturation surface coverage, Γ^∞, to obtain the final profile $c(z, \Gamma^\infty) = \int_0^{\Gamma^\infty} dc(z, \Gamma)$.

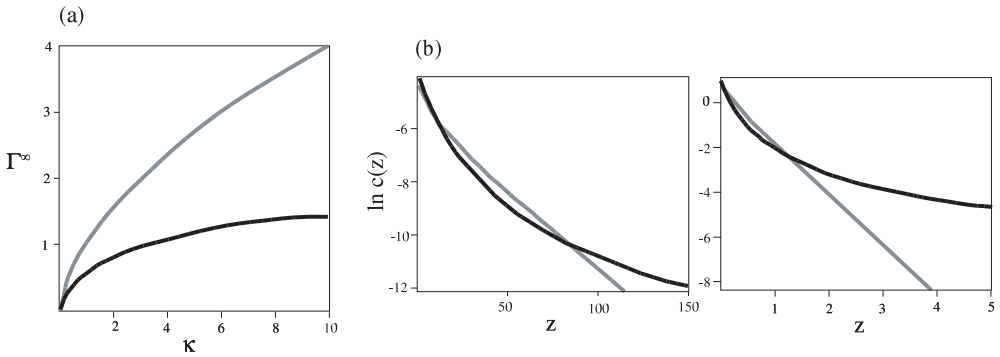

Figure 11. Results of Barford *et al* [186] for irreversible adsorption (black curves) compared to equilibrium (grey curves). Scales are arbitrary. (a) Total surface coverage Γ^{∞} as a function of κ, a dimensionless measure of monomer sticking energy. (b) Density profile c as a function of distance from the surface. $\kappa = 0.1$ and 5 shown on the left and right, respectively. Reproduced from [186].

The results of Barford *et al* [186] for irreversible adsorption compared to equilibrium self-consistent mean-field theory are illustrated in figure 11. The asymptotic surface coverage was found to be less than the equilibrium value (see figure 11(a)). Relative to the equilibrium density profile $c(z)$, the irreversible profile was larger at small and large z but smaller for intermediate z values (see figure 11(b)). Another prediction is that the final profiles depend on sticking energies, though results for very high sticking energies should be interpreted with caution since the equilibrium self-consistent theory predicts $\Gamma^{\infty} \to \infty$ for infinite chain–surface sticking energy (see figure 11(a)). In a subsequent work by Barford and Ball [187] the condition of frozen density profiles was relaxed and only the density at the interface was assumed to remain frozen. The final conclusions remained very similar.

Douglas *et al* [17] modelled irreversible adsorption by simulating a random sequential adsorption process [188]. In this work chains were visualized as deformable droplets. Initially, when a chain arrives at a bare surface, each droplet adsorbs onto a certain maximum cross-sectional area. As available surface area for adsorption becomes scarce, in order for late-arriving chains to adsorb it was assumed droplets deform by reducing their cross-sectional areas parallel to the surface to fit into the empty space. In so doing, they become more extended into the bulk. Using this model a $P(f)$ distribution was generated whose shape is similar to the experimental one of figure 10(b).

Motivated by the experiment of [16, 17] on PMMA adsorption, O'Shaughnessy and Vavylonis [133, 134] attempted to calculate layer structure at the detail of distributions of loop sizes and contact fractions, $\Omega(s)$ and $P(f)$. In this scaling theory, early arriving chains formed a flattened surface monolayer while late arrivers were visualized to adsorb irreversibly onto the few available unconnected empty surface sites (see figure 12(a)). Following [133], if each chain–surface adhesion point involves n_{cont} attached monomers, then the surface density of free 'supersites' (unoccupied surface patches large enough to accommodate n_{cont} monomers) is $\rho_{\mathrm{super}} \approx \Delta\Gamma_{\mathrm{bound}}/n_{\mathrm{cont}}$ where $\Delta\Gamma_{\mathrm{bound}} \equiv \Gamma^{\infty}_{\mathrm{bound}} - \Gamma_{\mathrm{bound}}$ is the density of available surface sites and $\Gamma^{\infty}_{\mathrm{bound}}$ the asymptotic density of surface-bound monomers. As the surface approaches saturation, the separation between supersites $l_{\mathrm{sep}} \approx \rho_{\mathrm{super}}^{-1/2}$ becomes large and the minimum loop size s which can come down just connects two free supersites, i.e. $as^{3/5} = l_{\mathrm{sep}}$ whence $s = (n_{\mathrm{cont}}/a^2\Delta\Gamma_{\mathrm{bound}})^{5/6}$. Chains adsorbing at this stage end up as trains of n_{cont} monomers separated by loops of order s units (see figure 12(a)). The bound fraction of those chains is

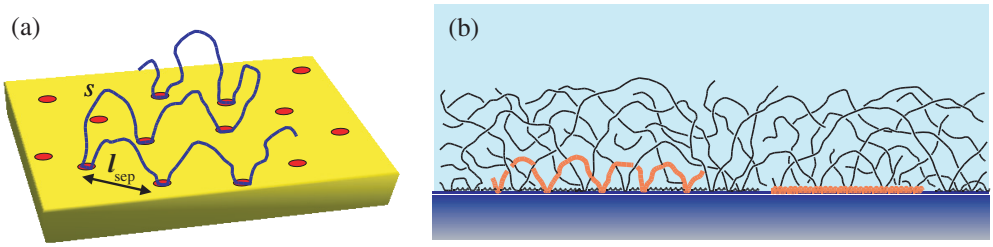

Figure 12. (a) Typical configuration of a chain adsorbed during the late stages, according to theory of [133, 134]. Such chains can adsorb onto free empty sites only (shown as discs) which are separated by l_{sep}. In so doing they form loops of s monomers, with $as^{3/5} = l_{sep}$. (b) Sketch of final irreversibly formed layer structure, as predicted in [133, 134]. The layer consists of two parts (one chain from each part is highlighted). (i) An inner region of flattened chains making $\approx\omega N$ contacts per chain, where ω is of order unity. (ii) A diffuse outer layer built up from chains each making $fN \ll N$ contacts with the surface. The values of f follow a distribution $P(f) \sim f^{-4/5}$. Each f value corresponds to a characteristic loop size for a given chain, $s \approx n_{cont}/f$.

$f = \partial\Delta\Gamma_{bound}/\partial\Delta\Gamma \approx n_{cont}/s$ for large s, where $\Delta\Gamma$ is the deviation from the asymptotic coverage Γ^{∞}. Integrating this process up to saturation gives

$$a^2\Delta\Gamma_{bound} = n_{cont}(a^2\Delta\Gamma/6)^6, \qquad P(f) = Af^{-4/5} \qquad (f \ll 1) \qquad (6)$$

where A is a constant of order unity. Equation (6) describes a tenuously attached outer layer (small f values) of late arriving chains, dressing the flattened inner layer (see figure 12(b)). Two notable features of $P(f)$ are a peak due to the outer layer at small f and a peak from the early stages centred at $f = \omega$. These results capture some essential features of the experimental data for PMMA as shown in figure 13. Interestingly, the predicted scaling forms for the loop distribution and density profile, $\Omega(s) \approx a^{-2}s^{-11/5}$ and $c(z) \sim z^{-4/3}$, are the same as those predicted for equilibrium layers (see equations (1) and (2)). However, a fundamental distinction is that the predicted distribution of bound fractions, figure 13(b), is very different to the equilibrium one shown in figure 3. This reflects the fact that, unlike equilibrium, all chains are no longer statistically identical; rather, there are infinitely many families, each parametrized by an f value.

5. Chemisorption

Chemisorption is characterized by very small values of the local monomer–surface reaction rate Q. Despite the importance of chemical adsorption in many applications, few experimental and theoretical works exist. Irreversibility effects are almost always relevant since chemical bond energies are virtually always much larger than kT.

5.1. Theory

The important feature of chemisorption is that due to the smallness of Q, chemical bond formation requires times which are typically longer than the relaxation time of the attached chain. Thus the reaction rate $k(s)$ of a monomer s units from a graft point is proportional to the equilibrium probability of finding this monomer on the surface, given the current constraints due to all chemical bonds formed at earlier times, see figure 14. The kinetics of single-chain chemisorption were first studied by Shaffer *et al* [46, 189] who focused on PMMA chemisorption onto Al. The form of $k(s)$ corresponding to theta solvent solutions was substituted into the master equation describing the evolution of the chain's loop distribution.

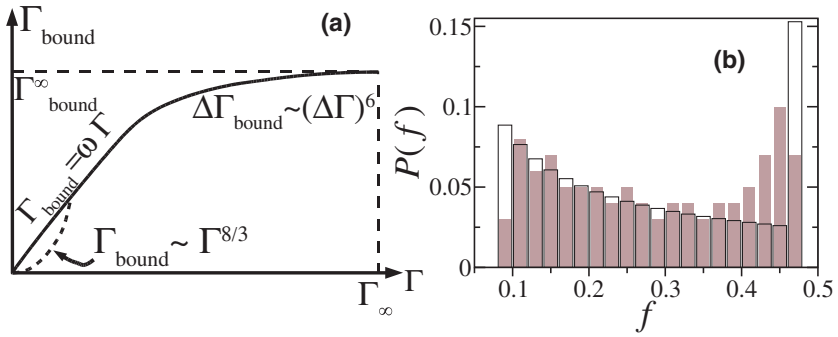

Figure 13. (a) Adsorbed polymer mass Γ versus surface-bound part Γ_{bound} as predicted by [133, 134]. For irreversible physisorption, early arriving chains have a fraction ω of their monomers bound to the surface and during early stages $\Gamma_{\text{bound}} \approx \omega\Gamma$. The early stage prediction for chemisorption is different, $\Gamma_{\text{bound}} \sim \Gamma^{8/3}$. The predicted form should be compared with the experimental results shown in figure 10(a). (b) Frequency histograms for bound mass fraction, f. Experiment (grey) from figure 10(b). Theory (empty), from predicted distribution $P(f) \sim f^{-4/5}$ with $f_{\min} < f < \omega$, where values for $f_{\min} = 0.09$ and $\omega = 0.47$ were derived from [16].

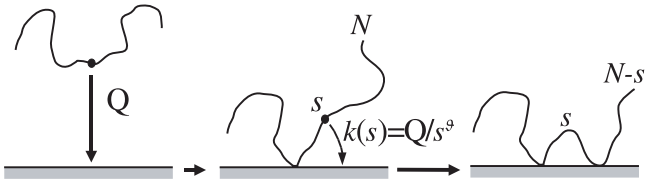

Figure 14. Single-chain chemisorption. A chain makes its first attachment with the surface and begins its adsorption process. The rate of first monomer attachment is proportional to Q, namely the reaction rate given the monomer touches the surface. While for physisorption subsequent monomer adsorption is diffusion controlled, for chemisorption the reaction rate $k(s)$ of the sth monomer away from the first attachment is proportional to the equilibrium monomer–surface conditional contact probability. For $s \ll N$, where N is the length of the tail, $k \approx Q/s^{\theta}$ where the exponent θ reflects equilibrium polymer statistics near an interface subject to the constraints imposed by earlier reactions.

Electronic structure calculations [189] indicated enhanced reaction rates for monomers neighbouring a graft point. Due to this local cooperative effect, the numerical solution of the master equation led to a process of chain zipping onto the surface growing outwards from the first attachments.

Ponomarev *et al* [167] used the bond-fluctuation model to simulate single-chain physisorption and chemisorption by varying monomer sticking energies and adsorption barrier heights. For chemisorption, in the limit of small Q they found $\tau_{\text{ads}} \sim N^{0.8\pm0.2}$ with a magnitude greater than the bulk chain relaxation time.

Scaling theory and asymptotic solutions of the chemisorbing chain master equation were developed by O'Shaughnessy and Vavylonis [133, 134]. Three general modes of adsorption were found, depending on the value of the exponent describing the decay of the reaction rate, $k(s) \sim s^{-\theta}$. For $\theta > 2$ the total reaction rate, $\int_0^{\infty} \mathrm{d}s\, k(s)$, is dominated by small loop sizes and this was found to lead to a zipping adsorption mode, the chain zipping down from the first attachment point. For $\theta < 1$, since the total reaction rate is dominated by large s large loops are more likely to form; this was found to lead to a process of uniform chain collapse, very different to zipping. The case $1 < \theta < 2$, named 'accelerated zipping', was

found to be intermediate between zipping and collapse; the pure zipping process is effectively short-circuited by the occasional adsorption of large loops which serve as nucleation points for further zipping. For non-attractive surfaces exact results were obtained for the exponent θ which can be expressed [134] in terms of other known critical exponents characterizing polymer networks [190, 191]. For dilute solutions the relation $\theta = 1 + \nu$ was obtained, where ν is Flory's exponent [81], giving $\theta = 8/5$ and $3/2$ for good and theta solvents, respectively. Thus the adsorption mode is accelerated zipping in both cases, and the adsorption time was found to be $\tau_{\text{ads}} \approx Q^{-1} N^{\theta-1}$.

O'Shaughnessy and Vavylonis [133, 134] also considered the kinetics of the build-up of a many-chain chemisorbed layer from dilute solution. Arguing that the timescale for single-chain adsorption was much smaller than the time for adsorbing chains to interfere with one another, they predicted a monolayer forms in the early stages. This is followed by a diffuse outer layer, attaching at the few available empty surface sites, just as for physisorption, figure 12. The final layer structure was thus of the same form, with two chain populations as in figure 12(b) and with the same loop and contact fraction distributions. However, the bound versus total mass relation differs for small coverage, $\Gamma_{\text{bound}} \sim \Gamma^{8/3}$ as in figure 13(a). The kinetics of layer formation are also very different: in physisorption diffusion-control was predicted to apply at all times, $\Gamma \sim t^{1/2}$, while for chemisorption $\Delta\Gamma \sim t^{-1/5}$ at long times.

5.2. Experiment

In contrast to physisorption, very few experiments have examined the fundamentals of polymer chemisorption. In principle however, since timescales are intrinsically much longer, the kinetics might be easier to probe. Schlenoff *et al* [192] studied PS with functional thiol groups along its backbone chemisorbing on gold from THF solution. Surface coverage was measured as a function of time using the quartz crystal microbalance and the degree of polymer functionalization, q, was varied. Pure PS did not adsorb; for $q = 1\%$ and MW $= 127\,000$, the asymptotic surface coverage was higher and was reached faster than when $q = 5\%$, MW $= 304\,000$. Lenk *et al* [193] studied thiol-functionalized PMMA chemisorption on gold. Similarly to the results of Schlenoff *et al* [192], it was found that less polymer adsorbed with increasing q. In every case, however, the final adsorbed amount was higher than the amount of unfunctionalized PMMA physisorbed onto gold. The final layer was found to contain unreacted thiols. Tsao *et al* [194] studied thiol-functionalized PDMS adsorption onto gold from dichloromethane. Similarly to [192, 193] less polymer adsorbed with increasing q. However, unlike the PMMA system [193] the final layer did not contain unreacted thiols except for the case $q = 1$. These thiol experiments are difficult to interpret at present since thiols not only chemisorb via their S group, but are also very powerful physisorbers onto gold [195]. In reality, therefore, a complex mixture of simultaneous physisorption and chemisorption is involved. It has also been suggested that they may self-associate in solution [192].

Cosgrove *et al* [196] studied the simultaneous physisorption and chemisorption of poly(methylsiloxane) on Al by Fourier-transform infrared specroscopy measuring total adsorbed mass as a function of polymer concentration in the bulk. Higher final coverages were found with increasing bulk concentration for a fixed adsorption time of one week. Physisorption processes rapidly formed a layer on the surface in less than an hour while chemisorption processes continued for days. For this system it was found that less mass was adsorbed when, prior to the experiment, the surface was initially exposed to a solution of the same polymer at lower concentrations. Qualitative agreement with this experiment was found in a lattice Monte Carlo model developed in [197, 198]. The simultaneous physisorption and chemisorption of poly(hydrogen methylsiloxane) on quartz and porous silica was studied by

neutron reflectometry and small angle neutron scattering in [199]. Adsorption was allowed to proceed for approximately one day at different temperatures. It was found that at higher temperatures the final layer had a more extended density profile and the total coverage was higher than at lower temperatures.

6. Concentration effects: irreversible adsorption from melts and semi-dilute solutions

In this section we review irreversible layer formation from polymer melts and solutions at finite concentration. This is a common situation arising in many applications involving reinforcement of polymer–solid or polymer–polymer interfaces [2, 6, 12, 200] where, for example, surfaces may be functionalized by various types of coupling agents [6, 201, 202]. In general, interfacial adsorption from melts and concentrated solutions may arise from either physical or chemical interactions. Clearly, the behaviour of chains in the immediate vicinity of a surface is relevant and such effects have been probed in experiments studying non-equilibrium polymer dynamics in thin melt films in contact with surfaces [177, 203, 204]. Here we do not review this large and developing rersearch field.

6.1. Physisorption: the Guiselin brush

Theory. Guiselin [55] proposed the following experimental procedure to study irreversible polymer adsorption from melts. He considered the situation where a melt is exposed to a surface so attractive to the polymer chains that they adsorb instantaneously and irreversibly. This can be realized in practice for very strong physisorption (e.g. strong hydrogen bonding). Assuming that chain configurations are equilibrated before the melt is brought in contact with the surface, then adsorption results in the irreversible freezing in of the equilibrium configurations of the chains which touch the surface. Given the ideal chain statistics in a polymer melt [81], the resulting loop distribution was found to be

$$\Omega(s) \approx 1/s^{3/2}, \qquad (s < N^{1/2}). \tag{7}$$

Here Ω is proportional to the probability that a random walk originating at the surface makes its first return to the surface after s steps. Guiselin proposed measuring this distribution by washing away unattached chains with a good solvent (see figure 15). This results in a swollen and stretched polydisperse brush with a density profile [55]

$$a^3 c(z) \approx (a/z)^{2/5}, \qquad (z < h = aN^{5/6}), \tag{8}$$

where h is layer height. An important difference between Guiselin's layer and equilibrium layers in dilute solutions (see equation (1)) is in the value of the total surface coverage, $\Gamma = \int_a^\infty \mathrm{d}z\, c(z)$. For equilibrium layers, from equation (1) one obtains $\Gamma \approx a^{-2}$ for $\epsilon > kT$. For the Guiselin brush on the other hand, most monomers in the melt within the coil radius $aN^{1/2}$ from the surface belong to chains which became attached. This leads to much higher surface coverages, $\Gamma \approx N^{1/2}a^{-2}$. If the above melt experiment is repeated in a semi-dilute solution of polymer volume fraction ϕ, Guiselin predicted that a fraction of order unity of monomers within the coil radius [81] $R \approx aN^{1/2}\phi^{-1/8}$ from the surface will become attached. This was shown by Marques and Joanny [205] to lead to a surface coverage

$$a^2\Gamma \approx (R/a)\phi \approx N^{1/2}\phi^{7/8}, \tag{9}$$

from which the melt case is recovered by setting $\phi = 1$ (see also [206]). For distances larger than the bulk correlation length of the semi-dilute solution, $z > a\phi^{-3/4}$, the density profile after removal of unattached chains was predicted to decay as $z^{-2/5}$ as in equation (8).

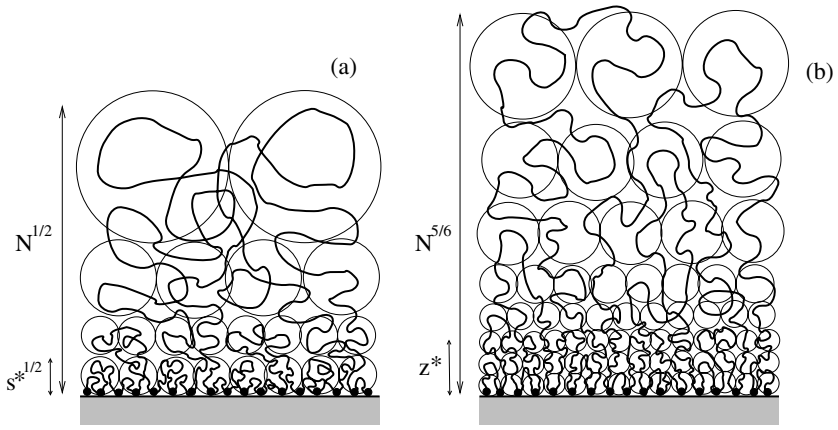

Figure 15. Irreversibly adsorbed layers from polymer melts. Theoretically predicted structures for physisorption and chemisorption are rather similar except at small scales. (a) Hierarchical loop structure after adsorption from the melt. For slow chemisorption [209] successive loop size scales are frozen in as their critical density is reached. Beyond this their formation would force chain stretching and hence is strongly suppressed. After time t the loops bigger than $s^* \sim 1/(Qt)^2$ get frozen in. For irreversible physisorption [55] by comparison all loop sizes freeze immediately. The end result is the same loop distribution but with s^* essentially one unit. (b) The experiment proposed by Guiselin [55] entails swelling the adsorbed structure shown in (a) with solvent and washing away unattached melt chains. The blob structure of the swollen layer in good solvent is shown. It consists of two regions separated at $z^* \sim s^{*3/5}$ corresponding to loop size s^* [55, 209], each region having a different density profile. For irreversible physisorption from a melt there is no inner region.

The structure of Guiselin's brush in contact with a polymer solution has been studied theoretically by Aubouy and Raphaël [207] and experimentally by Auroy and Auvray [208]. Adhesion properties have been reviewed by Léger *et al* [11].

Numerical simulations. The kinetics of irreversible physisorption from a semi-dilute solute were studied by Monte Carlo simulations by Zajac and Chakrabarti [120] assuming instantaneous and irreversible adsorption of monomers upon contact with the surface (values of N employed were 50, 100, and 200). It was found that for long times the surface coverage reached values consistent with an approximate law $\Gamma \sim N^{0.38}\phi^{0.38}$. The density profile of the adsorbed chains within the semi-dilute solution (i.e. without removing unattached chains) appeared to decay more slowly than $z^{-2/5}$. The first moment of the profile was found to increase as $\phi^{0.20\pm0.03}N^{0.81\pm0.05}$. It was found that the layer consisted of two regions: a loop-dominated inner region and a tail-dominated outer region.

Jia and Lai [210] used the bond-fluctuation Monte Carlo model to study instantaneous and irreversible polymer adsorption from semi-dilute solutions. In contrast to Zajac and Chakrabarti [120] they found that Γ asymptotes its long time value with a stretched exponential time dependence. Their results for layer height of the swollen layer were consistent with Guiselin's prediction in equation (8), though the chain lengths which were used were too short to probe the density profile ($N \leqslant 50$). They observed loop and tail regions similarly to [120].

Experiment. Experimentally, Cohen-Addad [211] and Cohen-Addad and Dujourdy [212] established that large surface coverages can be obtained in adsorption from melts. These studies involved hydrogen bonding of PDMS melts of various molecular weights onto fumed

silica particles. The particles were dispersed in the melt for varying periods of time. After washing away unattached chains with solvent, drying, and weighing, Γ was extracted as a function of N. For large enough times, equation (9) was satisfied with $\phi = 1$. However the asymptotic surface coverage was obtained after a very long time (weeks). These slow kinetics were interpreted within a model in which water molecules are initially adsorbed onto silica and prevent PDMS monomers from adsorbing; the kinetics was thus controlled by the diffusion of water molecules away from the surface [212–214]. Other models have also been suggested [215].

Auvray *et al* [216, 217] used small angle neutron scattering to study physisorption of PDMS onto silica through strong hydrogen bonding. Samples were prepared by immersing porous silica in a PDMS melt or a semi-dilute solution of PDMS in dichloromethane for a few days. The samples were then washed with dichloromethane and measured. By varying both N and the concentration of the semi-dilute solution, their measurements of surface coverages were in good agreement with equation (9). Measurements of the density profile for adsorption from a melt showed layer heights consistent with $h \sim N^{5/6}$ and evidence was found that the density profile could indeed decay as a power law.

Durning *et al* [218] used neutron reflectivity to study physisorption of PMMA from melts onto flat surfaces of hydroxylated quartz via hydrogen bonding. The melt was spin-cast onto the quartz plates and annealed for different time periods at 165 °C. Unbound chains were subsequently washed with benzene after cooling and the sample was measured. The total irreversibly adsorbed amount Γ was found to increase with annealing time, reaching a plateau after a few days. Since the process of spin-casting does not immediately generate equilibrium chain configurations at the interface, the dependence of Γ on annealing time was interpreted to be due to slow equilibration processes occurring at the interface during annealing. For the largest annealing times a scaling $\Gamma \sim N^{0.47\pm0.05}$ was found, consistent with equation (9). Their measurements of the density profile of the swollen layer were consistent with a power law decay, with an exponent whose value was about twice the predicted value of equation (8), while measured layer heights were smaller, $h \sim N^{0.72\pm0.03}$.

Marzolin *et al* [219] also used neutron reflectivity to study hydrogen-bonding of PDMS and deuterated PDMS (dPDMS) onto silicon wafers. Wafers were incubated in a PDMS melt for 12–24 h at 110 °C and unattached chains were rinsed by solvent (deuterated toluene for PDMS and octane for dPDMS). Measurements of density profiles for dPDMS showed good agreement with Guiselin's prediction, equation (8), but PDMS layers appeared to be less swollen.

The above experiments raise two important issues which deserve further study: (1) Guiselin's thought experiment which envisions the instantaneous freezing-in of equilibrium melt configurations in practice may require annealing over large timescales [218] for many experimental realizations. If the Guiselin predictions are to apply, this timescale, which depends on these unknown chain dynamics, must be large enough for any non-equilibrium configurations generated at the interface during melt deposition to have disappeared. (2) After swelling by solvent, one expects desorption–readsorption events and slow chain movements. This will eventually transform equation (8) into the equilibrium profile of equation (1).

6.2. Chemisorption: the slow Guiselin brush

Since chemical bond formation requires many surface–monomer collisions, chemisorption from melts can be thought of as a slow version of Guiselin's case which involved immediate bond formation. This process has been studied theoretically by O'Shaughnessy and Vavylonis [209]. Single-chain chemisorption kinetics was analysed in a similar way to that for

dilute solutions (section 5.1). The chief difference is the reaction exponent θ determining the surface reaction rate $k(s)$ of the sth monomer from a graft point (see figure 14). The exponent θ now represents ideal melt statistics due to screening of excluded volume interactions [81] leading to a value $\theta = 1/2$. Values of θ less than unity lead to *collapse* kinetics, during which each loop splits into two daughter loops of approximately equal size, very different to zipping mode. Since the lifetime of a loop of length s is $\tau_s \approx 1/\int_0^s \mathrm{d}s'\, k(s') \approx 1/(Qs^{1/2})$, by time t the maximum loop size which could have survived is $s^* = 1/(Qt)^2$. Thus at time t a single chain consists roughly of $\sim N/s^*$ loops of size s^*.

The single-chain collapse kinetics can only be realized for very dilute reactive chains in a bulk of identical but unreactive chains. When all chains are functionalized, it was shown in [209] that uninterrupted single-chain collapse does not proceed to completion. The reason is that if all $1/N^{1/2}$ chains per surface site were able to collapse independently, each would generate N/s^* loops of size s^* by time t, giving a net density $\approx N^{1/2}/s^*$. This would exceed the critical level, $1/s^{*1/2}$, beyond which adsorbed loops would have to be stretched [220]. In [209] it was assumed that loops are generated up to the critical density and no further. This leads to a layer which at any time consists of two parts: (i) an outer layer of frozen large loops at the critical density, and (ii) an inner layer of loops which have not yet collapsed. If reactions are stopped at t_{final} and the layer is swollen with solvent, the predicted layer height is $h = aN^{5/6}$ and the swollen layer has two regions with different density profiles $c(z)$: $c(z) \sim z^{*-2/5}$ for $z < z^*$ and $c(z) \sim z^{-2/5}$ for $z^* < z < h$ where $z^* = (Qt_{\mathrm{final}})^{-5/3}$. Note that the outer layer has the same power law profile and height as Guiselin's, equation (8), but the inner part is different.

7. Discussion

The experimental studies of strong physisorbing systems from solution in [16, 17] have identified an important layer property, namely the distribution of chain bound fractions, $P(f)$. Features of this fundamental layer characteristic may be more accessible to experiment than density profiles. In the appendix it was shown that for equilibrium layers in the long chain limit this distribution has a sharp peak at a value of f of order unity. Theoretically, then, the equilibrium layer consists of tightly bound and statistically identical chains, with the exception of a few more weakly attached chains (which however determine layer height). This general picture is supported by computer simulations [73, 101] which show that in practice for finite length chains the peak of $P(f)$ may be rather broad. The experimental discovery of a qualitatively very different and broad $P(f)$ for the strongly physisorbing PMMA-oxidized silicon system [16, 17] has demonstrated that such non-equilibrium layers comprise many classes of chain, each with its own f value corresponding to its time of arrival at the surface. In particular, a large subpopulation consists of weakly bound late arriving chains. The existence of a broad $P(f)$ is supported by theories addressing irreversible adsorption [17, 133, 134].

A promising approach for future experiments would be to probe $P(f)$ and its dynamics for less sticky systems which exhibit measurable ageing effects, such as PS on oxidized silicon [128, 129, 135]. It would be interesting to test what the initial $P(f)$ is in this case and if it does tend to relax towards equilibrium. During this relaxation process, the late arriving, weakly bound chains will progressively become more attached to the surface. Since weakly bound chains are presumably more easily displaced by bulk chains, it is possible that it is the relaxation process of $P(f)$ which underlies the slowing down of exchange rates with increasing ageing in many of the displacement experiments (see section 3.3).

Another promising future probe of processes in non-equilibrium layers lies in measurements of the dynamics of the lateral size of individual chains. As the chains which build up the layer flatten down onto the surface, theory has suggested that their initial size is of the order of the bulk size, $R \sim N^{3/5}$. In equilibrium layers however, theoretical arguments [100] support a picture in which most chains have a lateral size $R \sim N^{1/2}$ with the exception of a small fraction of weakly attached chains extending far into the bulk. This leads one to expect a process of chain shrinkage during layer ageing by a factor which may typically be of order unity. This change could be measurable with smart chain labelling.

Recently, Zhao and Granick [221] measured chain diffusion coefficients, D, as a function of surface coverage, Γ. They employed PEO chains with MW $= 10\,800$ adsorbed onto rather weakly attractive surfaces for which they estimated $\epsilon \approx 0.5\ kT$. They found that D was enhanced when the surface coverage increased towards what seemed to be the chain overlap threshold. But for layers whose coverage was far above this limit, they observed a large reduction in D. An interesting question motivated by this experiment is understanding how the curve $D(\Gamma)$ is modified with increasing surface stickiness.

The differing structures of the equilibrium and non-equilibrium layers should have important consequences for layer mechanical properties and interactions between layers. In the picture of [133, 134] the scaling of the density profile is the same for fully formed equilibrium and irreversibly formed layers. Now the interactions between two polymer-covered surfaces are believed to depend primarily on the density profiles [30, 146, 147]. Thus, when two such surfaces are brought into contact using a surface force apparatus [52], for example, this suggests force profiles should be qualitatively similar regardless of whether the polymer layers formed reversibly or irreversibly. Since the equilibrium layer chains rearrange themselves relatively rapidly, differences may manifest themselves at long times or very high forces when significant chain rearrangements can occur [48, 51, 52], leading to chain bridging and other complex effects. On the other hand adhesion properties may be very different in the two cases. Suppose a polymer layer is brought into contact with an elastomer or a polymer melt which is subsequently cooled [11]. Even though equilibrium and irreversible layers have similar loop distributions, the statistics of surface-chain attachments are very different (see sections 2.2 and 4.2). Consider a loop size s large enough to efficiently couple the surface to the bulk phase. For an equilibrium layer, this loop belongs to a chain having order N contacts with the surface; for an irreversibly formed layer the number of contacts is of order N/s, since the loop distribution for a given chain is roughly monodisperse. This suggests the equilibrium layer may produce a significantly stronger interface, though the details are complex and depend on the mode of fracture [12].

Finally, the process of polymer chemisorption remains largely unexplored experimentally and many possibilities for future work exist. While many chemisorbing systems may in practice involve some degree of simultaneous physisorption, there are also certain simplifications since the chemisorption process is very slow and often very close to the clean limit of complete irreversibility. Future research on the structure of chemisorbed layers promises to yield important insights into the many chemisorption-based applications involving reinforcement of polymer interfaces and adhesion.

Acknowledgment

This work was supported by the National Science Foundation under grant no DMR-9816374.

Appendix. Calculation of equilibrium distribution of bound fractions, $P^{\mathrm{eq}}(f)$

In this appendix we calculate $P^{\mathrm{eq}}(f)$ for a chain of length N in an equilibrium layer based on the statistics of loops and tails. We will make the approximation that the partition function $Z(n|N)$ of a chain of length N making n contacts with the surface (i.e. having two tails and $n-1$ loops) is the product of $n+1$ 'one-step' loop and tail weighting factors (see the end of the appendix for a self-consistency argument).

Definition of partition functions

Denoting by $W_{\mathrm{t}}(s|N)$ and $W_{\mathrm{l}}(s|N)$ the weighting factor for a tail and loop of size s, respectively, we have

$$Z(n|N) = \int_0^N \mathrm{d}t_1 \int_0^N \mathrm{d}t_2 \prod_{i=1}^{n-1}\left[\int_0^N \mathrm{d}s_i\right]\delta\left(N - t_1 - t_2 - \sum_{i=1}^{n-1} s_i\right) \times W_{\mathrm{t}}(t_1|N)W_{\mathrm{t}}(t_2|N)\prod_{i=1}^{n-1} W_{\mathrm{l}}(s_i|N). \tag{A.1}$$

The authors of [31, 100] evaluated the scaling forms of the partition functions $Z_{\mathrm{l}}(s|N)$ and $Z_{\mathrm{t}}(s|N)$ of loops and tails in the layer, respectively, which generate the self-similar equilibrium density profile. Thus the properties of W_{t} and W_{l} in equation (A.1) must be such that

$$\begin{aligned} Z_{\mathrm{t}}(s|N) &= W_{\mathrm{t}}(s|N)\sum_{n=1}^{\infty}\bar{Z}(n|N-s), \\ Z_{\mathrm{l}}(s|N) &= W_{\mathrm{l}}(s|N)\sum_{n=1}^{\infty}\sum_{m=1}^{\infty}\int_0^{N-s}\mathrm{d}s_1\,\bar{Z}(n|s_1)\bar{Z}(m|N-s-s_1), \end{aligned} \tag{A.2}$$

where $\bar{Z}$, defined similarly to equation (A.1), is the partition function for a chain with just one tail (its other end being in contact with the surface). We now make the ansatz that W_{l} and W_{t} have the same power law scaling as Z_{l} and Z_{t}, respectively, and we will later verify self-consistently that equation (A.2) is indeed satisfied in the limit $N \to \infty$. Using the results of [31, 100] we thus consider $W_{\mathrm{l}}(s|N) = \mu^s A_{\mathrm{l}}\eta_l(s|N)$ and $W_{\mathrm{t}}(s|N) = \mu^s A_{\mathrm{t}}\eta_t(s|N)$. Here A_{l} and μ are constants of order unity, $A_{\mathrm{t}} \approx N^{(\gamma-\nu)/4\nu}$, and

$$\begin{aligned} \eta_l(s|N) &\approx \begin{cases} s^{-1-2\nu} & (s \ll s^*) \\ s^{*-1-2\nu}(s^*/s)^{1+5\nu+\gamma} & (s \gg s^*) \end{cases} \\ \eta_t(s|N) &\approx \begin{cases} s^{*-1}(s^*/s)^{1-(\gamma-\nu)/2} & (s \ll s^*) \\ s^{*-1}(s^*/s)^{1+2\nu} & (s \gg s^*) \end{cases} \qquad s^* \equiv N^{1/(2\nu)}. \end{aligned} \tag{A.3}$$

The functions η_l and η_t are normalized to unity, $\gamma \approx 1.16$ is the susceptibility exponent [81], s is continuous, and a small-s cut-off at s of order unity is understood.

Calculation of $Z(n|N)$

We introduce a new variable M in equation (A.1) which allows us to simplify it by Laplace transforming $M \to E$ as follows:

$$Z(n|N) = \mu^N A_{\mathrm{t}}^2 A_{\mathrm{l}}^{n-1}\,\Xi_N(n|N),$$

$$\Xi_M(n|N) \equiv \int_0^M \mathrm{d}t_1 \int_0^M \mathrm{d}t_2 \prod_{i=1}^{n-1}\left[\int_0^M \mathrm{d}s_i\right]\delta\left(M - t_1 - t_2 - \sum_{i=1}^{n-1} s_i\right) \times \eta_t(t_1|N)\eta_t(t_2|N)\prod_{i=1}^{n-1}\eta_l(s_i|N). \tag{A.4}$$

Since Ξ_M is a convolution over loop and tail lengths, one has

$$\begin{aligned}\Xi_E(n|N) &= [\eta_t(E|N)]^2[\eta_l(E|N)]^{n-1} \\ &= \mathrm{e}^{(n-1)\ln\eta_l(E|N)+2\ln\eta_t(E|N)} \\ &\approx \mathrm{e}^{(n-1)[\eta_l(E|N)-1]+2\ln\eta_t(E|N)} \qquad (E \ll 1),\end{aligned} \tag{A.5}$$

where we used the fact that for $E \ll 1$, one has $\eta_l(E|N) \to 1$. Because the quantity $\eta_l(E|N) - 1$ appearing in equation (A.5) is small-scale dependent (due to the fact that the exponent $1 + 2\nu$ in equation (A.3) is larger than two), it is more natural to evaluate instead the Laplace transform of the distribution $\Xi'_Y(n|N)$, where

$$Y \equiv M - (n-1)\,\bar{s}_\mathrm{l} - 2\bar{s}_\mathrm{t}, \qquad \bar{s}_\mathrm{l} \equiv \int_0^\infty \mathrm{d}s\, s\, \eta_l(s|N), \qquad \bar{s}_\mathrm{t} \equiv \int_0^\infty \mathrm{d}s\, s\, \eta_t(s|N) \approx s^*. \tag{A.6}$$

Note that the loop size $\bar{s}_\mathrm{l}$ is of order unity and depends on the cut-off of η_l in equation (A.3), while $\bar{s}_\mathrm{t} \sim N^{1/(2\nu)}$. As will become clear below (equation (A.10)) in the limit $M \to \infty$ the probability of negative Y values becomes zero. For $M \gg 1$ one can neglect negative Y and after using equation (A.5) one has

$$\Xi'_E(n|N) = \Xi_E(n|N)\mathrm{e}^{E(n-1)\bar{s}_\mathrm{l}+2E\bar{s}_\mathrm{t}} = \mathrm{e}^{(n-1)[\eta_l(E|N)-1+E\bar{s}_\mathrm{l}]+2[\ln\eta_t(E|N)+E\bar{s}_\mathrm{t}]} \qquad (E \ll 1), \tag{A.7}$$

where E is now conjugate to Y. Laplace transforming equation (A.3) one obtains the following expressions for the quantities appearing in equation (A.7):

$$\begin{aligned}1 - \eta_l(E|N) - E\bar{s}_\mathrm{l} &\approx \begin{cases} E^{2\nu} & (1 \ll E^{-1} \ll s^*) \\ s^{*-2\nu}(Es^*)^2 & (E^{-1} \gg s^*) \end{cases} \\ -\ln\eta_t(E|N) - E\bar{s}_\mathrm{t} &\approx \begin{cases} -(Es^*) & (1 \ll E^{-1} \ll s^*) \\ (Es^*)^{2\nu} & (E^{-1} \gg s^*). \end{cases}\end{aligned} \tag{A.8}$$

Using equation (A.8) in equation (A.7) one finds that the loop and tail contributions dominate for large and small E, respectively:

$$\Xi'_E(n|N) \approx \begin{cases} \mathrm{e}^{-B(n-1)E^{2\nu}} & (1 \ll E^{-1} \ll s^*) \\ \mathrm{e}^{-C(Es^*)^{2\nu}} & (E^{-1} \gg s^*) \end{cases} \tag{A.9}$$

where B and C are positive constants of order unity. In deriving equation (A.9) we have considered $f = n/N$ of order unity since, self-consistently, the probability of very small f values is very small (see equation (3)). Laplace inverting one has

$$\Xi'_Y(n|N) \approx \frac{N}{Y^{1+2\nu}}\,\zeta\left(\frac{Y}{n^{1/(2\nu)}}\right), \qquad \zeta(x) \to \begin{cases} 1 & (x \gg 1) \\ 0 & (x \ll 1), \end{cases} \tag{A.10}$$

where $\zeta(x)$ is a cut-off function. This distribution has a peak at $Y \approx n^{1/(2\nu)}$, a long tail for large Y, and is exponentially small for $Y \ll n^{1/(2\nu)}$. One thus obtains $Z(n|N)$ by using $Y \to N - (n-1)\bar{s}_\mathrm{l} - 2\bar{s}_\mathrm{t}$ in equation (A.10) and substituting into equation (A.4):

$$Z(n|N) \approx \mu^N A_\mathrm{t}^2 A_\mathrm{l}^{n-1}\frac{N}{[N-(n-1)\bar{s}_\mathrm{l}-2\bar{s}_\mathrm{t}]^{1+2\nu}}\,\zeta\left(\frac{N-(n-1)\bar{s}_\mathrm{l}-2\bar{s}_\mathrm{t}}{n^{1/(2\nu)}}\right). \tag{A.11}$$

This expression will immediately yield $P^{\mathrm{eq}}(f)$ (see below).

Self-consistency check and the value of A_1

We now show that our choice of weighting factors in equation (A.1) leads to loop and tail partition functions in equation (A.2) which are consistent with the findings of [31, 100] provided the normalization constant A_1 in the one-loop distribution function obeys certain constraints.

Consider first Z_t in equation (A.2). Repeating the above calculations of equations (A.1)–(A.10) for the case of a chain with one tail, one can show that $\bar{Z}(n|N) = \mu^N A_t A_1^{n-1} \bar{\Xi}_N(n|N)$, where $\bar{\Xi}_N$ has the same scaling structure as Ξ_N. Using the definition of $W_t(s|N)$ one thus has from equation (A.2)

$$Z_t(s|N) = \mu^N A_t^2 \eta_t(s|N) \sum_{n=1}^{\infty} \bar{\Xi}_{N-s}(n|N-s) \mathrm{e}^{(n-1)\ln A_1}. \tag{A.12}$$

Now suppose $\mathrm{e}^{N \ln A_1} \gg 1$, in which case the exponential favours large values of n. Since $\bar{\Xi}_{N-s}$ has a sharp cut-off for n values of order $(N-s)/\bar{s}_1$, the sum in equation (A.12) is then dominated by n values of this order. This would imply $Z_t(s|N) \sim \mathrm{e}^{-(s \ln A_1)/\bar{s}_1}$ is exponentially suppressed for larger s, inconsistent with the tail partition function derived in [31, 100]. The latter has a power law dependence on s (note that Z_t in equation (A.2) involves a sum over configurations of the whole chain and unlike W_t it involves a factor μ^N instead of μ^s). Thus, self-consistency requires that the value of A_1 is such that $\mathrm{e}^{N \ln A_1}$ is non-diverging as $N \to \infty$.

The case $\mathrm{e}^{N \ln A_1} \ll 1$ is also inconsistent; then the chain partition function, $Z(n|N)$, would be largest for n values much less than N (see equation (A.11)). This would imply that the mean bound fraction is much less than unity, inconsistent with the equilibrium layer for which a fraction of order unity of the adsorbed mass contacts the surface.

Overall, we conclude $\mathrm{e}^{N \ln A_1}$ is of order unity. In this case the sum in equation (A.12) is to leading order independent of s and thus $Z_t(s|N)$ has the same scaling as $\eta_t(s|N)$; this is consistent with the results of [31, 100]. Repeating the above arguments for the case of loops, and considering $\mathrm{e}^{N \ln A_1}$ of order unity, one finds $Z_l(s|N)$ has the same scaling with respect to s as $\eta_l(s|N)$. This is also consistent with [31, 100].

The distribution of bound fractions

The probability $P(n|N)$ to have n loops is obtained from $P(n|N) = Z(n|N)/\sum_{n=1}^{N} Z(n|N)$. Since the bound fraction is $f = n/N$, then using $P^{\mathrm{eq}}(f)\,\mathrm{d}f = P(n|N)\,\mathrm{d}n$ and $\nu \approx 3/5$ one has

$$P^{\mathrm{eq}}(f) \approx X \mathrm{e}^{fN \ln A_1} \frac{N^{-1/5}}{(f_{\max} - f)^{11/5}} \rho\left[(f_{\max} - f)N^{1/6}\right], \tag{A.13}$$

where X is a normalization constant, $f_{\max} \approx 1/\bar{s}_1$, and ρ is defined in equation (3). Since $\mathrm{e}^{N \ln A_1}$ is of order unity, from equation (A.13) one recovers equation (3) of the main text.

Self-consistency of equation (A.1)

The assumption of independent loop statistics is consistent with the hypothesis of ideal lateral blob statistics at every scale in the adsorbed layer [100]. The approximation is also self-consistent in the sense that the probability that a chain makes two overlapping loops of the same size s at the same spot on the surface is small. The number of successive loops n needed to make a loop of size of order s or larger is $n \approx \int_s^N \mathrm{d}s'\,\Omega(s') \approx s^{6/5}$. During these steps the chain would have performed a random walk on the surface of size $n^{1/2} \approx s^{3/5}$. Thus the origin of the next loop of size s is just outside the region occupied by the previous loop of the same size.

References

[1] Wool R P 1994 *Polymer Interfaces: Sructure and Strength* (Cincinnati: Hanser Gardner Publications)
[2] Wu S 1982 *Polymer Interface Adhesion* (New York: Dekker)
[3] Wicks Z W, Jones F N and Pappas S P 1999 *Organic Coatings: Science and Technology* 2nd edn (New York: Wiley–Interscience)
[4] Russel W B, Saville D A and Schowalter W R 1989 *Colloidal Dispersions* (Cambridge: Cambridge University Press)
[5] Mittal K L (ed) 1996 *Polymer Surface Modification: Relevance to Adhesion* (Utrecht: VSP)
[6] Edwards D C 1990 *J. Mater. Sci.* **25** 4175–85
[7] Hogg R 1999 *Colloids Surf.* **146** 253–63
[8] Brown Patrick O and David B 1999 *Nat. Genet. Suppl.* **21** 33–7
[9] Malmsten M (ed) 2003 *Biopolymers at Interfaces* (*Surfactant Science Series* vol 110) 2nd edn (New York: Dekker)
[10] Granick S, Kumar S K, Amis E J, Antonietti M, Balazs A C, Chakraborty A K, Grest G S, Hawker C, Janmey P, Kramer E J, Nuzzo R, Russell T P and Safinya C R 2003 *J. Polym. Sci.* B **41** 2755–93
[11] Léger L, Raphaël E and Hervet H 1999 *Adv. Polym. Sci.* **138** 185–225
[12] Creton C, Kramer E J, Brown H R and Hui C-Y 2001 *Adv. Polym. Sci.* **156** 53–136
[13] Laible R and Hamann K 1990 *Adv. Colloid Interface Sci.* **13** 65–99
[14] Halperin A, Tirrel M and Lodge T P 1992 *Adv. Polym. Sci.* **100** 31
[15] Tirell M and Levicky R 1997 *Curr. Opin. Solid State Mater. Sci.* **2** 668–72
[16] Schneider H M, Frantz P and Granick S 1996 *Langmuir* **12** 994–6
[17] Douglas J F, Schneider H M, Frantz P, Lipman R and Granick S 1997 *J. Phys.: Condens. Matter* **9** 7699–718
[18] van der Beek G P, Cohen Stuart M A, Fleer G J and Hofman J E 1991 *Macromolecules* **24** 6600–11
[19] Frantz P and Granick S 1992 *Langmuir* **8** 1176–82
[20] Hlady V and Buijs J 1996 *Curr. Opin. Biotechnol.* **7** 72–7
[21] Israelachvili Jacob N 2003 *Intermolecular and Surface Forces* 3rd edn (San Diego, CA: Academic)
[22] Joesten M D and Schaad L J 1974 *Hydrogen Bonding* (New York: Dekker)
[23] Semenov A N, Bonet-Avalos J, Johner A and Joanny J F 1996 *Macromolecules* **29** 2179
[24] de Gennes P G 1981 *Macromolecules* **14** 1637–44
[25] de Gennes P G 1987 *Adv. Colloid Interface Sci.* **27** 189–209
[26] Eisenriegler E 1983 *J. Chem. Phys.* **79** 1052–64
[27] Eisenriegler E, Kremer K and Binder K 1982 *J. Chem. Phys.* **77** 6297–320
[28] de Gennes P G and Pincus P 1983 *J. Physique Lett.* **44** L241–6
[29] de Gennes P G 1982 *C. R. Acad. Sci. Paris* II **294** 1317–20
[30] Aubouy M, Guiselin O and Raphael E 1996 *Macromolecules* **29** 7261–8
[31] Semenov A N and Joanny J-F 1995 *Europhys. Lett.* **29** 279–84
[32] Cosgrove T, Heath T G, Ryan K and Crowley T L 1987 *Macromolecules* **20** 2879
[33] Cosgrove T, Heath T G, Phipps J S and Richardson R M 1991 *Macromolecules* **24** 94–8
[34] Cosgrove T 1990 *J. Chem. Soc. Faraday Trans.* **86** 1323–32
[35] Auvray L and Cotton J P 1987 *Macromolecules* **20** 202–7
[36] Rennie A R, Crawford R J, Lee E M, Thomas R K, Crowley T L, Roberts S, Qureshi M S and Richards R W 1989 *Macromolecules* **22** 3466–75
[37] Hone J H E, Cosgrove T, Saphiannikova M, Olbey T M, Marshall J C and Crowley T L 2002 *Langmuir* **18** 855–64
[38] Lee L T, Guiselin O, Farnoux B and Lapp A 1991 *Macromolecules* **24** 2518–22
[39] Guiselin O, Lee L T, Farnoux B and Lapp A 1991 *J. Chem. Phys.* **95** 4632–40
[40] Sun X, Bouchaud E, Lapp A, Farnoux B, Daoud M and Jannink G 1988 *Europhys. Lett.* **6** 207
[41] Fleer G J, Cohen Stuart M A, Scheutjens J M H M, Cosgrove T and Vincent B 1993 *Polymers at Interfaces* (London: Chapman and Hall)
[42] Kremer K 1986 *J. Physique* **47** 1269
[43] de Gennes P G 1988 *Molecular Conformation and Dynamics of Macromolecules in Condensed Systems* ed N Nagasawa (Amsterdam: Elsevier) pp 315–31
[44] Chakraborty A K, Shaffer J S and Adriani P M 1991 *Macromolecules* **24** 5226–9
[45] Chakraborty A K and Adriani P M 1992 *Macromolecules* **25** 2470–3
[46] Shaffer J S and Chakraborty A K 1993 *Macromolecules* **26** 1120–36
[47] Adriani P M and Chakraborty A K 1993 *J. Chem. Phys.* **98** 4263–74
[48] Johner A and Semenov A N 2002 *Eur. Phys. J.* E **9** 413–6

[49] Sommer J-U 2002 *Eur. Phys. J.* E **9** 417–9
[50] Granick S 2002 *Eur. Phys. J.* E **9** 421–4
[51] Raviv U, Klein J and Witten T A 2002 *Eur. Phys. J.* E **9** 425–6
[52] Raviv U, Klein J and Witten T A 2002 *Eur. Phys. J.* E **9** 405–12
[53] Luckham P F and Klein J 1985 *Macromolecules* **18** 721–8
[54] Raviv U, Tadmor R and Klein J 2001 *J. Phys. Chem.* B **105** 8125–34
[55] Guiselin O 1992 *Europhys. Lett.* **17** 225–30
[56] O'Shaughnessy B and Vavylonis D 1999 *Macromolecules* **32** 1785–96
[57] O'Shaughnessy B and Vavylonis D 1999 *Europhys. Lett.* **45** 638–44
[58] O'Shaughnessy B 1998 *Theoretical and Mathematical Models in Polymer Science* ed A Grosberg (New York: Academic) chapter 5, pp 219–75
[59] O'Shaughnessy B and Vavylonis D 2000 *Phys. Rev. Lett.* **84** 3193–6
[60] O'Shaughnessy B and Vavylonis D 2000 *Eur. Phys. J.* E **1** 159–77
[61] O'Shaughnessy B and Vavylonis D 1999 *Europhys. Lett.* **45** 653–8
[62] Ligoure C and Leibler L 1990 *J. Physique* **51** 1313
[63] Kramer E J 1995 *Isr. J. Chem.* **35** 49
[64] O'Shaughnessy B and Sawhney U 1996 *Phys. Rev. Lett.* **76** 3444–7
[65] Fredrickson G H 1996 *Phys. Rev. Lett.* **76** 3440–3
[66] O'Shaughnessy B and Sawhney U 1996 *Macromolecules* **29** 7230–9
[67] Fredrickson G H and Milner S T 1996 *Macromolecules* **29** 7386–90
[68] Netz R R and Andelman D 2003 *Phys. Rep.* **380** 1–95
[69] Netz R R and Andelman D 2001 *Oxide Surfaces* ed J A Wingrave (New York: Dekker) pp 115–55
[70] Clement F and Johner A 2000 *C. R. Acad. Sci. Paris* IV **1** 1135–42
[71] Eisenriegler E 1993 *Polymers Near Surfaces* (Singapore: World Scientific)
[72] Bouchaud E and Daoud M 1987 *J. Physique* **48** 1991–2000
[73] Zajac R and Chakrabarti A 1996 *J. Chem. Phys.* **104** 2418–37
[74] de Joannis J, Park C-W, Thomatos J and Bitsanis I A 2001 *Langmuir* **17** 69–77
[75] de Joannis J, Ballamudi R K, Park C-W, Thomatos J and Bitsanis I A 2001 *Europhys. Lett.* **56** 200–6
[76] Cifra P 2003 *Macromol. Theory Simul.* **12** 270–5
[77] Scheutjens J M H M and Fleer G J 1979 *J. Phys. Chem.* **83** 1619–35
[78] Scheutjens J M H M and Fleer G J 1980 *J. Phys. Chem.* **84** 178–90
[79] Scheutjens J M H M, Fleer G J and Cohen Stuart M A 1986 *Colloids Surf.* **21** 285
[80] van der Linden C C and Leermakers F A M 1992 *Macromolecules* **25** 3449–53
[81] de Gennes P G 1985 *Scaling Concepts in Polymer Physics* (Ithaca, NY: Cornell University Press)
[82] Jones I S and Richmond P 1977 *J. Chem. Soc. Faraday Trans.* II **73** 1062–70
[83] Johner A, Bonet-Avalos J, van der Linden C C, Semenov A N and Joanny J F 1996 *Macromolecules* **29** 3629
[84] Fleer G J, van Male J and Johner A 1999 *Macromolecules* **32** 825–44
[85] Fleer G J, van Male J and Johner A 1999 *Macromolecules* **32** 845–62
[86] Blokhuis E M, Skau K I and Avalos J B 1989 *J. Chem. Phys.* **119** 3483–94
[87] Avalos J B, Mackie A D and Diez-Orrite S 2004 *Macromolecules* **37** 1124–1133
Avalos J B, Mackie A D and Diez-Orrite S 2004 *Macromolecules* **37** 1143–51
[88] Ploehn H J, Russel W B and Hall C K 1988 *Macromolecules* **21** 1075–85
[89] Ploehn H J and Russel W B 1989 *Macromolecules* **22** 266–76
[90] Barnett K G, Cosgrove T, Vincent B, Sissons D S and Cohen-Stuart M 1981 *Macromolecules* **14** 1018
[91] van der Beek G P, Cohen Stuart M A and Cosgrove T 1991 *Langmuir* **7** 327
[92] Kobayashi K, Sugimoto S, Yajima H, Araki K, Imamura Y and Endo R 1990 *Bull. Chem. Soc. Japan* **53** 2018–24
[93] Robb I D and Smith R 1974 *Eur. Polym. J.* **10** 1005
[94] Kawaguchi M, Hayakawa K and Takahashi A 1980 *Polym. J.* **12** 265–70
[95] Kawaguchi M, Mikura M and Takahashi A 1984 *Macromolecules* **17** 2063–5
[96] Cosgrove T, Vincent B, Crowley T L and Cohen Stuart M A 1984 *ACS Symp. Ser.* **240** 147
[97] Kato T, Nakamura K, Kawaguchi M and Takahashi A 1981 *Polym. J.* **13** 1037
[98] Kawaguchi M and Takahashi A 1983 *Macromolecules* **16** 1465–9
[99] Klein J and Luckham P F 1986 *Macromolecules* **19** 2005
[100] Semenov A N and Joanny J-F 1995 *J. Physique* II **5** 859–76
[101] Wang Y and Rajagopalan R 1996 *J. Chem. Phys.* **105** 696
[102] de Gennes P G 1989 *New Trends in Physics and Physical Chemistry of Polymers* ed L-H Lee (New York: Plenum) pp 9–18

[103] de Gennes P G 1985 *C. R. Acad. Sci. Paris* II **301** 1399
[104] de Gennes P G 1988 *C. R. Acad. Sci. Paris* II **306** 183
[105] de Gennes P G 1988 *C. R. Acad. Sci. Paris* II **306** 739
[106] Baschnagel J, Johner A and Joanny J-F 1998 *Eur. Phys. J.* B **6** 45–55
[107] Zheng X, Sauer B B, Van Alsten J G, Schwarz S A, Rafailovich M H, Sokolov J and Rubinstein M 1995 *Phys. Rev. Lett.* **74** 407
[108] Cohen Stuart M A and de Keizer A 2001 *Oxide Surfaces* ed J A Wingrave (New York: Dekker) pp 157–99
[109] Bychuk O and O'Shaughnessy B 1994 *J. Physique* II **4** 1135–56
[110] Wang Y, Rajagopalan R and Mattice W L 1995 *Macromolecules* **28** 7058–63
[111] Hasegawa R and Doi M 1997 *Macromolecules* **30** 3086–9
[112] Milchev A and Binder K 1996 *Macromolecules* **29** 343
[113] Lai P-Y 1996 *Macromol. Theory Simul.* **5** 255–68
[114] Liu H and Chakrabarti A 1999 *Polymer* **40** 7285–93
[115] Ponomarev A L, Sewell T D and Durning C J 2000 *J. Polym. Sci.* B **38** 1146–54
[116] Carlos Hernandez A and Fichthorn K A 2001 *Int. J. Hydrogen Energy* **26** 1307–12
[117] Wang Y, Rajagopalan R and Mattice W L 1995 *Phys. Rev. Lett.* **74** 2503–6
[118] Lai P-Y 1995 *J. Chem. Phys.* **103** 5742–55
[119] Lai P-Y 1994 *Phys. Rev.* E **49** 5420
[120] Zajac R and Chakrabarti A 1995 *Phys. Rev.* E **52** 6536–49
[121] Takeuchi H 1999 *Macromol. Theory Simul.* **8** 391–401
[122] Pefferkorn E, Carroy A and Varoqui R 1985 *J. Polym. Sci. Polym. Phys. Edn* **23** 1997
[123] Pefferkorn E, Haouam A and Varoqui R 1989 *Macromolecules* **22** 2677–82
[124] Varoqui R and Pefferkorn E 1990 *Prog. Colloid Polym. Sci.* **83** 96
[125] Pefferkorn E 1999 *J. Colloid Interface Sci.* **216** 197–220
[126] Pefferkorn E, Carroy A and Varoqui R 1985 *Macromolecules* **18** 2252
[127] Pefferkorn E, Haouam A and Varoqui R 1988 *Macromolecules* **21** 2111–6
[128] Frantz P and Granick S 1991 *Phys. Rev. Lett.* **66** 899–902
[129] Frantz P and Granick S 1994 *Macromolecules* **27** 2553–8
[130] Cohen Stuart M A, Fleer G J and Scheutjens J M H M 1984 *J. Colloid Interface Sci.* **97** 515–25
[131] Cohen Stuart M A, Fleer G J and Scheutjens J M H M 1984 *J. Colloid Interface Sci.* **97** 526–35
[132] van der Beek G P, Cohen Stuart M A, Fleer G J and Hofman J E 1989 *Langmuir* **5** 1180–6
[133] O'Shaughnessy B and Vavylonis D 2003 *Phys. Rev. Lett.* **90** 056103
[134] O'Shaughnessy B and Vavylonis D 2003 *Eur. Phys. J.* E **11** 213–30
[135] Schneider H M and Granick S 1992 *Macromolecules* **25** 5054
[136] Dijt J C, Stuart M A, Cohen G J and Fleer 1994 *Macromolecules* **27** 3219–28
[137] Brandrup J, Immergut E H, Grulke E A, Abe A and Bloch D R 1999 *Polymer Handbook* 4th edn (New York: Wiley)
[138] Mubarekyan E and Santore M M 2001 *Macromolecules* **34** 4978–86
[139] Fu Z and Santore M 1998 *Macromolecules* **31** 7014–22
[140] Fu Z and Santore M 1999 *Macromolecules* **32** 1939–48
[141] Mubarekyan E and Santore M M 2001 *Macromolecules* **34** 7504–13
[142] Trens P and Denoyel R 1993 *Langmuir* **9** 519–22
[143] Johnson H E and Granick S 1990 *Macromolecules* **23** 3367
[144] Frantz P and Granick S 1995 *Macromolecules* **28** 6915–25
[145] Soga I and Granick S 1998 *Macromolecules* **31** 5450–5
[146] de Gennes P G 1982 *Macromolecules* **15** 492–500
[147] Rossi G and Pincus P A 1989 *Macromolecules* **22** 276
[148] Klein J and Rossi G 1998 *Macromolecules* **31** 1979–88
[149] Mendez-Alcaraz J M, Johner A and Joanny J F 1998 *Macromolecules* **31** 8297–304
[150] Hu H-W and Granick S 1990 *Macromolecules* **23** 613–23
[151] Ruths M, Israelachvilli J N and Ploehn H J 1997 *Macromolecules* **30** 3329–39
[152] Granick S, Patel S and Tirrell M 1986 *J. Chem. Phys.* **85** 5370–1
[153] Ruths M, Yoshizawa H, Fetters L J and Israelachvilli J N 1996 *Macromolecules* **29** 7193–203
[154] Duval M 2000 *Macromolecules* **33** 7862–7
[155] Porsch B and Sundelof L-O 1995 *Macromolecules* **28** 7165–70
[156] Boils D and Hair M L 1993 *J. Colloid Interface Sci.* **157** 19–23
[157] Marra J and Hair M L 1988 *Macromolecules* **21** 2349–55
[158] Johnson H E, Douglas J F and Granick S 1993 *Phys. Rev. Lett.* **70** 3267

[159] Johnson H E and Granick S 1992 *Science* **255** 966
[160] Schneider H M, Granick S and Smith S 1994 *Macromolecules* **27** 4714–20
[161] Schneider H M, Granick S and Smith S 1994 *Macromolecules* **27** 4721–5
[162] Dijt J C, Cohen Stuart M A and Fleer G J 1994 *Macromolecules* **27** 3229–37
[163] Pan W, Bossmann S, Durning C J and Turro N J 1995 *Macromolecules* **28** 7284–8
[164] de Gennes P G 1985 *J. Physique Lett.* **44** L639–42
[165] Doi M and Edwards S F 1986 *The Theory of Polymer Dynamics* (Oxford: Clarendon)
[166] Shaffer J S 1994 *Macromolecules* **27** 2987–95
[167] Ponomarev A L, Sewell T D and Durning C J 2000 *Macromolecules* **33** 2662–9
[168] van Eijk M C P, Cohen Stuart M A, Rovillard S and De Coninck J 1998 *Eur. Phys. J.* B **1** 233–44
[169] Konstadinidis K, Prager S and Tirrell M 1992 *J. Chem. Phys.* **97** 7777–80
[170] Sukhishvili S A, Chen Y, Muller J D, Gratton E, Schweizer K S and Granick S 2000 *Nature* **406** 146
[171] Sukhishvili S A, Chen Y, Muller J D, Gratton E, Schweizer K S and Granick S 2002 *Macromolecules* **35** 1776–84
[172] Bae S C, Xie F, Jeon S and Granick S 2001 *Curr. Opin. Solid State Mater. Sci.* **5** 327–32
[173] Maier B and Radler J O 1999 *Phys. Rev. Lett.* **82** 1911–4
[174] Maier B and Radler J O 2000 *Macromolecules* **33** 7185–94
[175] Fredrickson G H and Andersen H C 1984 *Phys. Rev. Lett.* **53** 1244–7
[176] Keddie J L, Jones R A L and Cory R A 1994 *Faraday Discuss.* **98** 219–30
[177] Jones R A L 1999 *Curr. Opin. Colloid Interface Sci.* **4** 153–8
[178] de Gennes P G 1991 *C. R. Acad. Sci.* II **313** 1117–22
[179] de Gennes P G 1992 *Pure Appl. Chem.* **64** 1585–8
[180] Zheng X, Rafailovich M H, Sokolov J, Strzhemechny Y, Schwarz S A, Sauer B B and Rubinstein M 1997 *Phys. Rev. Lett.* **79** 241–4
[181] Semenov A N 1998 *Phys. Rev. Lett.* **80** 1908–11
[182] Semenov A N and Johner A 2003 *Eur. Phys. J.* E **12** 469–80
[183] Deutsch J M 1985 *Phys. Rev. Lett.* **54** 56
[184] Deutsch J M 1987 *J. Physique* **48** 141
[185] Semenov A N and Rubinstein M 1998 *Eur. Phys. J.* B **1** 87–94
[186] Barford W, Ball R C and Nex C M M 1986 *J. Chem. Soc. Faraday Trans.* 1 **82** 3233–44
[187] Barford W and Ball R C 1987 *J. Chem. Soc. Faraday Trans.* 1 **83** 2515–23
[188] Talbot J, Tarjus G, Van Tassel P R and Viot P 2000 *Colloids Surf.* **165** 287–324
[189] Shaffer J S, Chakraborty A K, Tirrell M, Davis H T and Martins J L 1991 *J. Chem. Phys.* **95** 8616–30
[190] Duplantier B 1989 *J. Stat. Phys.* **54** 581–680
[191] De'Bell K and Lookman T 1993 *Rev. Mod. Phys.* **65** 87–113
[192] Schlenoff J B, Dharia J R, Xu H, Wen L and Li M 1995 *Macromolecules* **28** 4290–5
[193] Lenk T J, Hallmark V M and Rabolt J F 1993 *Macromolecules* **26** 1230–7
[194] Tsao M-W, Pfeifer K-H, Rabolt J F, Castner D G, Haussling L and Ringsdorf H 1997 *Macromolecules* **30** 5913–9
[195] Lavrich D, Wetterer S, Bernasek S and Scoles G 1998 *J. Phys. Chem.* B **102** 3456–65
[196] Cosgrove T, Prestidge C A and Vincent B 1990 *J. Chem. Soc. Faraday Trans.* **86** 1377–82
[197] Cosgrove T, Prestidge C A, King A M and Vincent B 1992 *Langmuir* **8** 2206–9
[198] King S M and Cosgrove T 1993 *Macromolecules* **26** 5414
[199] Cosgrove T, Patel A, Webster J R P and Zarbakhsh A 1993 *Langmuir* **9** 2326–9
[200] Kraus G 1965 *Reinforcement of Elastomers* (New York: Wiley)
[201] Clegg D W and Collyer A A (ed) 1986 *Mechanical Properties of Reinforced Thermoplastics* (London: Elsevier)
[202] Pireaux J J, Bertrand P and Bredas J L (ed) 1992 *Polymer–Solid Interfaces* (Bristol: Institute of Physics Publishing)
[203] Jones R L, Kumar S K, Ho D L, Briber R M and Russell T P 1999 *Nature* **400** 146–9
[204] Forrest J A 2002 *Eur. Phys. J.* E **8** 261–6
[205] Marques C M and Joanny J F 1988 *J. Physique* **49** 1103–9
[206] Johner A, Joanny J-F and Rubinstein M 1993 *Europhys. Lett.* **22** 591
[207] Aubouy M and Raphaël E 1994 *Macromolecules* **27** 5182–6
[208] Auroy P and Auvray L 1996 *Macromolecules* **29** 337–42
[209] O'Shaughnessy B and Vavylonis D 2003 *Europhys. Lett.* **63** 895–901
[210] Jia L-C and Lai P-Y 1996 *J. Chem. Phys.* **105** 11319–25
[211] Cohen Addad J P 1989 *Polymer* **30** 1820–3
[212] Cohen Addad J P and Dujourdy L 1998 *Polym. Bull.* **41** 253–60

[213] Cohen Addad J P and de Gennes P G 1994 *C. R. Acad. Sci. Paris* II **319** 25–30
[214] Cohen Addad J P and Morel N 1995 *C. R. Acad. Sci. Paris* IIb **320** 455–61
[215] Levresse P, Feke D L and Manas-Zloczower I 1998 *Polymer* **39** 3919–24
[216] Auvray L, Auroy P and Cruz M 1992 *J. Physique* I **2** 943–54
[217] Auvray L, Cruz M and Auroy P 1992 *J. Physique* II **2** 1133–40
[218] Durning C J, O'Shaughnessy B, Sawhney U, Nguyen D, Majewski J and Smith G S 1999 *Macromolecules* **32** 6772–81
[219] Marzolin C, Auroy P, Deruelle M, Folkers J P, Léger L and Menelle A 2001 *Macromolecules* **34** 8694–700
[220] de Gennes P G 1980 *Macromolecules* **13** 1069
[221] Zhao J and Granick S 2004 *J. Am. Chem. Soc.* **126** 6242–3